Title: Death and Proliferation of Lymphocytes in Immune Response and Tumor Cells Are Controlled by pH Balance

Wei-ping Zeng, Ph.D.[1,*]

[1]Therazwimm Corporation, 3128 Ferguson Road, Huntington, WV 25705

[*]Correspondence: Wei-ping Zeng, Therazwimm Corporation, 3128 Ferguson Road, WV 25705, USA. E-mail: weipingzengny@gmail.com

Abstract

Many biological processes are controlled by cell death and proliferation. The present study found that cellular pH was positively correlated with proliferation but negatively with apoptosis. Alkaline treatments enhanced lymphocyte proliferation in response to antigen challenge in vivo and in vitro cultures, whereas acid treatments induced apoptosis. Low pH was incompatible with the survival of highly proliferating cells, and the susceptibility to the acid-induced death was determined significantly by the proliferative status of the lymphocytes. Likewise, alkaline treatments maintained tumor cell proliferation whereas acid treatments induced apoptosis. These data support a unified theory of regulation of cell death and proliferation where a cellular pH balance controls both events, and the mitochondria act as pH-stats. Accordingly, the Warburg effect is viewed as necessary for proliferating cells to have a high cellular pH environment to accelerate proliferation and avoid acid-induced death.

Introduction

Cell death and proliferation play fundamental roles in numerous biological processes throughout the life cycle of an organism. In humans and animals, cell death and proliferation are key to understanding immune response and tumorigenesis, two biological processes that are of particular importance for the health of an individual. An immune response commences with clonal expansion of antigen specific lymphocytes and ends with the death of most of the expanded antigen specific lymphocytes by mitochondrion- and death receptor-initiated apoptosis. (*1-4*). On the other hand, the basic features of tumor cells are unrestricted proliferation and resistance to cell death. In tumor cells, the genes for apoptosis inhibitors Bcl-2, Bcl-x Mcl-1 are over expressed or amplified whereas genes for apoptosis activators Bim, Puma, Bad and Bax are suppressed or deleted. (*5*). While the death receptor-initiated apoptosis is sufficient for the cell death under certain circumstances, it often needs to be linked to the mitochondrial process to complete cell killing such that mitochondria play a central role in apoptosis. (*6-8*).

On the other hand, mammalian cell proliferation is primarily controlled at the "restriction point" by retinoblastoma family proteins (pRB). (*9, 10*). Mitogenic signals generated by external stimulants at the cell membrane are transduced to the nucleus to induce the transcription of D and E type cyclin genes, which leads to the activation of cyclin-dependent kinases CDK4/6 and CDK2, respectively. The activated CDKs phosphorylate the pRB proteins. (*11-14*). Phosphorylated pRB proteins dissociate with E2F family transcription factors to allow the latter to activate target gene expression, which in turn causes the cell to pass the restriction point, transition from G1 to S phase and commit to completing the cell cycle. (*15, 16*).

Although apoptosis and G1/S transition appear to be controlled by separate pathways, the increased demand of energy and substrates for anabolic metabolism of the proliferating cells suggests that mitochondria may positively regulate both apoptosis and proliferation. On the contrary, almost a century ago Otto Warburg observed that cell malignant transformation includes a precancerous phase, in which the cell must incur irreversible "injury of respiration" or "uncoupling of respiration and phosphorylation" and switch energy production to glycolysis followed by pyruvate fermentation and excretion of the fermentation waste product lactate (herein referred to as the glucose/lactate pathway). (*17, 18*). This phenomenon has come to be known as the "Warburg Effect", and later found to be shared by both tumor and normal proliferating cells. (*19-21*). However, the glucose/lactate pathway in the cytosol is not only inefficient for energy production, but also unlikely to contribute to anabolic metabolism. This is because in this pathway only 2 ATPs per glucose are produced as opposed to a net production of 32 ATPs by glycolysis followed by TCA cycle and oxidative phosphorylation in the mitochondrion; all atoms in the glucose are converted to lactate that cannot be further used by the cell and is excreted; and there is no net production of NADH or $FADH_2$ as potential reducing equivalents for biomass synthesis. (*22*). Intriguingly, unlike originally suggested by Warburg, mitochondria in most tumor cells and normal proliferating cells are not "injured" but functional. (*21, 23*). Given that most tumor microenvironments are poor in nutrients (*24*), it is puzzling why the inefficient glucose/lactate pathway predominates in the tumor cells.

In this study, it was found that cell proliferation positively whereas apoptosis negatively correlates with pH. Alkaline treatment enhanced cell proliferation whereas

acid treatment preferentially induced death of proliferating cells. These findings support a unified theory of cell fate determination that a cellular pH balance dictates whether a cell dies or proliferates, and the mitochondria as proton generators via carbohydrate catablolism act as "pH-stats". Thus, the Warburg effect or the turning down of mitochondrial energy production is viewed as necessary for highly proliferating cells to avoid low pH-induced death and create a high pH environment for accelerating proliferation.

Results

The current study stemmed from an unexpected finding of thymic atrophy in animals that received a test compound prepared in an acid solution. (Manuscript in preparation). Since thymus is one of a few organs in adults that maintain robust cell proliferation, this observation led to the investigation of whether pH regulates immune responses by affecting lymphocyte survival and proliferation in the draining lymph nodes (DLN) where immune responses to local antigen exposure take place.

Positive relationship between intracellular pH and lymphocyte proliferation

Experiments were performed to determine whether there is a natural correlation between cellular pH and proliferation. Lymph node cells were labeled with CFSE, and cultured either with IL-2 alone or IL-2 and anti-CD3 antibodies for the study of T cell proliferation, or alternatively with either IL-4 alone or IL-4 and the B cell mitogen LPS for the study of B cell proliferation. Lymphocyte proliferation was measured by serial dilution of the CFSE signals after each cell division, whereas the intracellular pH was measured by the fluorescence intensity of the pH indicator pHrodo™ Red AM that

inversely correlates with intracellular pH. Proliferating lymphocytes were detected even in cultures with IL-2 or IL-4 alone, indicating the pre-existence of proliferating cells prior to mitogenic stimulation. (Figure 1a and b). As expected, proliferating cells ($CFSE^{lo}$) increased with concurrent decrease of non-proliferating cells ($CFSE^{hi}$) after stimulation by anti-CD3 antibodies or LPS; and even the pre-existent proliferating cells underwent further divisions as evidenced by the decrease of the CFSE signals. (Figure 1a and b). Importantly, the highly proliferating cells that had undergone more than 3 divisions were almost exclusively in the cell populations of high intracellular pH, whereas cells that had fewer than 3 divisions were in cell populations of low intracellular pH. (Figure 1a and b). Within the highly proliferating cells, the higher numbers of cell divisions correlate with higher intracellular pH. (Figure 1a and b).

Effects of treatments with pH modifiers on the total number of MLN cells

To investigate whether lymphocyte survival and proliferation in an active immune response in vivo could be affected by acid and alkaline treatments, ovalbumin (OVA)-sensitized mice were intra-tracheally challenged with OVA, and the lung-draining lymph nodes mediastinal lymph nodes (MLN) were analyzed. In the first set of experiments, MLNs were collected from mice 3 days after the first OVA challenge and 1 day after a single treatment with saline or saline containing HOAc or HCl. In the second set of experiment, MLNs were collected 7 days after the initial challenge and 3 days after 3 treatments with saline or saline containing HOAc, HCl or NaOH. (Figure 2a and b, upper panels). The average numbers of total MLN were greatly reduced in HOAc-treated mice as compared with those of the saline-treated mice (0.75×10^7 vs. 4.5×10^7, or 84% reduction) in the fist set of experiments. In the second set of experiments in which MLNs

were collected at a later time, the reduction of total MLN cells in the HOAc-treated mice as compared with the saline-treated mice was also dramatic but less severe than in the first set of experiments (4.23 x 10^7 vs. 5.96 x 10^7, or 29% reduction), which suggested on-going replenishment of the MLNs with lymphocytes after the HOAc treatment. The total MLN cells were also significantly reduced in HCl-treated mice but less dramatic than in the HOAc-treated mice in either the first (4.0 x 10^7, or 12% reduction) or second (5.6 x 10^7, or 5.5% reduction) set of experiments. In contrast, treatment with NaOH increased total MLN cells (7.9 x 10^7, or 32% increase). (Figure 2a and b, lower panels). The differences in the total MLN cells were not due to differences in Treg cell populations because there were similar percentages of Treg cells in CD4 T cells among the different treatment groups. (Manuscript in preparation).

Effects of treatments with pH modifiers on different lymphocyte populations in MLNs

Total lymphocytes, CD4, CD8 T cells and B cells in MLNs were further analyzed. The majority of the total lymphocytes in the MLNs in the first set of experiments had relatively small sizes and low granularities, and were referred to as Lym1. In addition, some lymphocytes were of larger sizes and higher granularities, and were referred to as Lym2, which were likely lymphoblasts. (Figure 3a, upper right). The percentages of both the Lym1 and Lym2 in MLN cells were greatly reduced in the HOAc-treated mice as compared with those in the saline-treated mice (32.4% vs. 73.7% and 0.35% vs. 2.26% for Lym1 and Lym2, respectively). The percentage of Lym1 was also somewhat lower in the HCl-treated mice (68.3%), but the Lym2 percentage was similar 2.83%) to saline-treated mice. (Figure 3a, upper right). Within the Lym1 population, the percentages of CD4, CD8 T cells and B cells in the HOAc-treated mice were all lower than those of the

saline-treated mice (8.17% vs. 39.6%, 1.75% vs. 13.9%, and 22.2% vs. 42.5%, respectively), and similar reductions were also observed in the Lym2 lymphocytes (3.23% vs. 14.2%, 2.7% vs. 9.69%, and 46.9% vs. 62.6%). To lesser degrees, the percentages of CD4, CD8 T cells and B cells (13.4%, 8.2% and 44.8%, respectively) in Lym2 of the HCl-treated mice were also reduced. In contrast, within the Lym1 only the percentage of B cells (34.4%) of the HCl-treated mice was reduced. (Figure 3a, lower).

In the second set of experiments or at a later time of MLN collection, the Lym2 populations had expanded as compared with the first set of experiments, and the combined percentages of Lym1 and Lym2 were similar in all treatment groups, even in the HOAc-treated mice, again indicating replenishment of MLNs with lymphocytes. (Figure 3c, upper right). The relative proportions of Lym1 and Lym2 were similar among the saline, HCl and NaOH treatment groups. However, the proportion of the Lym2, which as shown in Figure 3c lower right panels consisted mostly of B lymphoblasts, in the HOAc-treated mice was greatly increased as compared with the saline-treated mice (38.7% vs. 8.10%). (Figure 3c, upper and lower right). This result shows that B lymphoblasts were less susceptible to depletion by HOAc than T lymphoblasts, therefore were selectively retained in the MLNs.

Within the Lym1 in the second set of experiments, the percentages of CD4 and CD8 T cells in the HOAc-treated mice were lower than those of the saline-treated mice (44.3% vs. 54.9% or 19.3% reduction, and 7.39% vs. 13.9% or 46.8% reduction), whereas the percentage of B cells were higher (43.8% vs. 27.3%), once again showing that B cells were less susceptible than T cells to depletion. The percentages of CD4, CD8 T cells and B cells in Lym1 of the HCl-treated mice were similar to those of the saline-

treated mice. In the NaOH-treated mice percentages of CD4 (45.2%) and CD8 (10.2%) were slightly reduced, whereas that of B cells (38.4%) was increased. (Figure 3c, lower left). Within the Lym2 populations, the reductions of the percentages of CD4 and CD8 T cells in the HOAc-treated mice were even greater than in Lym1 (0.8% vs. 6.91% or 88% reduction, and 0.35% vs. 4.21% or 91.7% reduction), consequently the percentage of B cells proportionally increased (93% vs. 84%). In contrast, the percentage distributions of CD4, CD8 T cells and B cells in Lym2 of the HCl- and NaOH-treated mice were similar to those of the saline-treated mice. (Figure 3c, lower right).

Thus, acid treatments reduced, whereas alkaline treatment increased, the number of MLNs cells during active immune responses. HOAc treatment appeared to exert stronger effects than HCl treatment. T cells were more susceptible than B cells to the acid-mediated depletion.

Effects of treatments with pH modifiers on cell proliferation in MLNs

The proliferative statuses of the lymphocytes in the MLNs were determined by their expression of Ki-67. Ki-67 is a widely used, dependable marker of proliferating cells; its level of expression positively correlates with rRNA and DNA synthesis. (*25*).

In the first set of experiments, the majority of the Lym1 cells expressed only low levels of Ki-67 but small percentages of the Lym1 cells expressed high levels of Ki-67. In the HOAc-treated mice, the percentage of Ki-67^{hi} Lym1 cells was less than half of that of the saline-treated mice (1.65% vs. 3.31%), the percentage of the Ki-67^{hi} Lym1 cells in the HCl-treated mice (2.92%) was also reduced. In the HOAc-treaed mice, even the percentage of Ki-67^{lo} cells in Lym1 was also reduced (32.9% vs. 80.4%), whereas the percentage of Ki-67^{lo} Lym1 cells in HCl-treated mice was similar to that of the saline-

treated mice. (Figure 3b). The Lym2 cells were overall more proliferative than the Lym1 cells. In the HOAc-treated mice the percentage of Ki-67^{hi} Lym2 cells was less than half of that of the saline-treated mice (27.2% vs. 54.5%), the percentage of Ki-67^{hi} Lym2 cells in HCl-treated mice (49.1%) was also reduced. (Figure 3b).

Thus, proliferating lymphocytes in the MLNs were preferentially depleted by acid treatments. Lymphocytes of high proliferative status were more susceptible to depletion than those of low proliferative status, which in turn were more susceptible than the non-proliferating cells.

Since B cells in MLNs were less susceptible to depletion by acid treatments, experiments were conducted to determine whether proliferative status of B cells nonetheless also correlates with susceptibility to depletion by acids. In the first set of experiments, in both the Lym1 and Lym2, the percentages of Ki-67^{hi} B cells were the lowest in HOAc-treated mice (1.58% and 37.9%, respectively), followed by those in HCl-treated mice (2.79% and 51.1%), and highest in the saline-treated mice. (3.91% and 62.6%). (Figure 3b).

In the second set of experiments, the percentages of Ki-67^{hi} Lym1 cells were lower in HCl- or HOAc-treated mice (2.42% and 2.67%), but higher in NaOH-treated mice (3.48%), than that of saline-treated mice (2.73%). The percentages of Ki-67^{hi} B cells in Lym1 were also lower in the HCl- or HOAc-treated mice (3.62% and 2.38%) than, but similar in the NaOH-treated mice (4.23%) to, that of the saline-treated mice (4.29%). (Figure 3d, upper panels). The percentage of Ki-67^{hi} Lym2 cells in HOAc-treated mice (25.3%) was lower, whereas that of NaOH-treated mice (42.2%) was higher, than that of saline-treated mice (34.9%). The percentages of Ki-67^{hi} B cells in Lym2

followed the same pattern, with those of saline-, HOAc- and NaOH-treated mice being 35.2%, 24.9% and 44.7%, respectively. The percentages of Ki-67^{hi} Lym2 and Lym2 B cells in the HCl-treated mice (34.9% and 35.5%) were similar to those of the saline-treated mice. (Figure 3d, lower). However, the mean fluorescence intensities of the Ki-67^{hi} Lym2 and Lym2 B cells of the HCl-treated mice, like those of the HOAc-treated mice, were much lower, whereas they were higher in NaOH-treated mice, than those of the saline-treated mice. (Figure 3e). Thus, acid treatments not only preferentially depleted Ki-67^{hi} cells but also lower their proliferative profiles, whereas alkaline treatment had the opposite effects.

Effects *of in vitro treatments with pH modifiers on proliferating lymphocytes*

Due to the complexity of the in vivo environment, it cannot be definitively determined whether the effects of in vivo treatments with the pH modifiers on MLN lymphocytes were direct or indirect. Further, the fluidity of the in vivo environment could mask the full effects of the pH modifiers. For example, circulating and/or newly activated lymphocytes could replenish the MLNs after lymphocyte depletion by acid treatments. Moreover, the kinetics of absorption and the subsequent transportation of the pH modifiers into and out of the MLNs are unknown. As such, the actual duration and concentrations of pH modifiers at which the pH modifiers acted in the MLNs could not be determined.

To bypass these complexities and better assess the full potentials of the pH modifiers, in vitro experiments were carried out, in which primary MLN cells were treated with saline or saline containing the pH modifiers in 100% FBS in a 37 ^{o}C water bath. Such in vitro cultures were designed to be free of interference by pH buffering

agents in common tissue culture system. As shown in Figure 4, the in vitro treatments with HCl or HOAc eliminated almost all Ki-67^{+} (Ki-67$^{hi\ and\ lo}$) cells in total lymphocytes, the CD4, CD8 T cells and B cells. In contrast, in vitro NaOH treatment more than tripled the percentages of Ki-67^{+} cells in total lymphocytes and CD8 T cells, and nearly tripled in the CD4 T cells and B cells. Thus, the in vitro results collaborated the in vivo observation that acid treatments preferentially depleted, whereas alkaline treatment increased, the proliferating lymphocytes. The in vitro treatments showed stronger effects than the in vivo treatments, which was likely due to higher concentration and longer time of action of the pH modifiers in the in vitro cultures than in the MLNs in vivo.

Low pH correlated with lymphocyte apoptosis

Having demonstrated a positive relationship between high pH and lymphocyte proliferation, further experiments were carried out to determine whether conversely low pH correlates with lymphocyte death by apoptosis. In steady state peripheral lymphocytes of unimmunized mice, about 5% of total lymphocytes were apoptotic, and a similar percentage of the cells were early apoptotic (Annexin V^{high} 7-AAD^{-}, see (*26*) for definition of early apoptotic cells), and various percentages of these two populations were found in B cells, CD4 and CD8 T cells. (Figure 5a). Since direct measurement of intracellular pH of apoptotic (dead) cells was impossible because of their leaky cell membranes, early apoptotic cells were analyzed as proxies. In all live lymphocyte populations, the early apoptotic cells were detected primarily in cells of low intracellular pH. (Figure 5b).

Apoptotic and early apoptotic cells were also detected in the peripheral lymphocytes that had been activated in vitro by anti-CD3 or LPS. (Figure 5c and e).

Treatments with HOAc in FBS caused over 70% of the cells become apoptotic, whereas the overall percentage of apoptotic cells after NaOH treatment was around 8% similar to that of the saline treated cells. (Figure 5 c and e). Regardless of the treatments, early apoptotic cells were detected almost exclusively in the pH low populations. (Figure 5d and f).

Finally, MLNs from mice sensitized and challenged with OVA, and in vivo treated with i.p. injection of saline, or saline containing HOAc or NaOH were studied. Similar small percentages (around 1%) of apoptotic cells were detected in the MLN cells of all treatment groups. (Figure 5g). Most of the MLN cells had relatively high pH, and small percentages of the cells were pH low. About half or more of the pH low MLN cells were early apoptotic. In contrast, only about 10 to 15% of the pH high MLN cells were early apoptotic with high levels of Annexin V staining. (Figure 5h). However, the intracellular pH values of these small percentages of early apoptotic cells in the pH high populations (Q1) were lower than those of their Annexin V low counterparts (Q4), as shown by their higher mean fluorescence intensities (MFI) of pH indicator. (Figure 5i).

Since apoptotic cells are quickly removed in vivo (*27*), the effects of pH modifiers on apoptosis would be better determined by in vitro experiments. After the MLN cells from OVA sensitized and challenged mice were treated with HOAc, more than 70% were apoptotic, whereas there were only 2.43% and 1.35% apoptotic cells after in vitro NaOH or saline treatment, respectively. (Figure 5j). In all treatment groups, early apoptotic cells were primarily found in the pH low populations. (Figure 5k).

Effects of treatments with pH modifiers on tumor cell viability and proliferation

Cell proliferation is a common basic feature of immune response and tumorigenesis. To determine weather the pH modifiers would have effects on tumor cells similar to those on proliferating lymphocytes, the human T and B cell leukemia cell lines Jurkat and Raji, respectively, were treated with saline or saline containing HCl, HOAc or NaOH in FBS. Compared with saline treatment, HCl and HOAc treatments greatly reduced the viabilities of the Jurkat (22.1% and 34.3% vs. 73/4%) and Raji (49.2% and 48.9% vs. 89.4%) cells. In contrast, NaOH treatment only slightly decreased the viabilities of Jurkat and Raji cells (70.4% and 76.2%, respectively). (Figure 6a). The tumor cells were further analyzed for Ki-67 expression. After saline treatments, the majorities of live Jurkat cells remained Ki-67^{+} (71.7%). However, few, if any, (<2%) live Jurkat cells after the HOAc treatment expressed Ki-67. In contrast, the percentage of Ki-67^{+} live Jurkat cells after NaOH treatment was similar to that after saline treatment. (Figure 6b, upper). In Raji cells, HOAc treatment dramatically reduced Ki-67^{hi} cells as compared with saline treatment (9.69% vs 41.3%). In contrast, Ki-67 expression after NaOH treatment was similar to that of saline treatment. (Figure 6b, lower).

Low pH correlated with tumor cell death by apoptosis

The tumor cells were further analyzed for death by apoptosis and intracellular pH. Apoptotic cells were about 40% to 60% for Jurkat cells and about 55% to 85% for Raji cells after treatments with saline or saline containing HOAc or NaOH in FBS. (Figure 7a and b, upper panels). It should be noted that the percentages of apoptotic dead cells in the saline and NaOH treatment groups were higher than what were determined in the viability tests by Trypan blue staining in Figure 6a. The additional apoptotic cell death was likely caused by the removal of the tumor cells from the FBS and incubation in

serum free buffers at 37°C and room temperature during pH indicator and Annexin V staining. Conversely, many early dead cells in the HOAc treatment groups had disintegrated during the staining processes. Nonetheless, regardless of the treatments, early apoptotic tumor cells were primarily in the pH low populations. (Figure 7a and b, lower panels). Some early apoptotic cells were also found in the pH high Jurkat cell populations. However, these pH "high" early apoptotic cells apparently had higher staining of the pH indicator hence lower pH than their non-apoptotic pH high counterparts. (Figure 7a).

Discussion

This article studies the impact of pH on the survival and proliferation of normal lymphocytes in an active immune response and in tumor cells. It was found that cell proliferation is positively whereas cell death by apoptosis is negatively correlated with pH. Therefore, cellular pH balance determines whether a cell proliferates or dies. When the balance tips towards higher pH, proliferation increases, when it tips lower the cell dies. In agreement, alkaline treatments enhanced cell proliferation whereas acid treatments induced death by apoptosis. Highly proliferative cells were more susceptible than modestly proliferating cells, which in turn were more susceptible than non-proliferating cells, to acid-induced cell death. Thus, a high pH environment is not only favorable for proliferation but also necessary for the survival of the proliferating cells.

Mitochondria are not only energy but also proton generators via aerobic respiration. Catabolizing 1 glucose molecule through glycolysis and mitochondrial pathways produces 6 CO_2, 10 $NADH_2^+$ and 2 $FADH_2$. CO_2 is converted to carbonic

acids in the cell by carbonic anhydrase, which produces protons. (*28, 29*). $NADH_2^+$ are fed to the electron transport chain to create mitochondrial membrane potential and proton gradient to drive ATP synthesis. However, up to 20 to 25% of mitochondrial respiration is uncoupled from ATP synthesis, which can also cause net increases of protons in the cell that can spill across mitochondrial outer membrane to cytosol. (*30, 31*). Consequently, if mitochondrial respiration were to increase to meet the heightened energy demand of proliferating cell, it would be incompatible with a high cellular pH environment for proliferation, but instead tip the cellular pH balance lower to trigger apoptosis. Indeed, glycolysis and glutaminolysis are characteristic of energy metabolism in proliferating cells. Glycolysis followed by lactate excretion produces no CO_2 and no net $NADH_2^+$ and FADH. In glutaminolysis, glutamine is deaminated to produce ammonia and glutamate. As found in many tumor cells, glutamate is often excreted from proliferating cells, (*32*), which together with ammonia production can increase intracellular pH. Glutamate can also be further metabolized and participate in the malate-aspartate shuttle to move protons from cytosol to mitochondria to raise cytosolic pH.

Thus, the Warburg effect could be the strategy of the proliferating, especially highly proliferating, cells to satisfy the requirement of a high cellular pH environment for proliferation and survival. This provides an alternative explanation for the Warburg effect to the theory that Warburg effect is required for satisfying increased demand for substrates of biomass synthesis. (*20, 33*). The biomass theory suggests that the use of the mitochondrial pathways for energy production might cause over production of ATP, which could inhibit glycolysis resulting in insufficient supply of glycolytic intermediates

for biomass synthesis. While both the pH balance and the biomass theories need to be validated by further experimentation, logically they are not mutually exclusive.

The Warburg effect is evolutionary conserved as similar phenomena are observed across species. For example, yeast growth accelerates as glucose concentration increases. However, when the yeast growth and glucose concentration reach critical points, the yeasts switch energy production from oxidative respiration to fermentation. This phenomenon is known as Crabtree effect. (*34, 35*). It is conceivable that the switch is necessary for the yeasts' survival because if oxidative respiration continues to increases, it could lower cellular pH to induce cell death. In bacteria, the Entner-Doudoroff glycolytic pathway is low efficient for energy production as it produces only 1 ATP per glucose, but counter intuitively it is much more common among aerobic and facultative than anaerobic bacteria, suggesting this pathway is needed to substitute for aerobic respiration. (*36*). Indeed, like the yeasts, bacteria switch to energetically inefficient metabolism when growth rate increases to a critical level. (*37*). Similarly, parasites that cause major parasitic diseases such as malaria, schistosomiasis, trypanosomiasis and leishmaniasis switch to glycolysis during the stages of their life cycles in mammalian hosts, likely to avoid cell death. (*38-40*).

The evolutionary conservation suggests that pH modifiers can be used to control not only immune response and tumorigenesis as shown in this study but also the survival and proliferation of pathogens. This is particularly important considering that the increase of antimicrobial resistance has become a major health threat. For example, the prevalence of vancomycin-resistant *Staph. aureus* (VRSA) has increased from 2% before 2006 to 7% in 2015-2020. (*41*). Based on the present study, new therapies can be

developed to use pH modifiers to tilt pH balance to induce cell death or to diminish propagation of pathogens regardless of their drug resistant abilities.

The present study provides potentially new ways to either enhance or suppress immune and/or inflammatory responses. In situations such as cancers and infectious diseases where there is insufficient protective immunity, pH modifiers that increase or resist the fall of pH could be used to promote lymphocyte proliferation therefore enhance immune and inflammatory responses against the infectious agents or cancer cells. In other situations where overzealous immune or inflammatory responses impair normal tissue structure and functions, pH modifiers that decrease pH or resist the rise of pH may be used to dampen the overzealous immune or inflammatory responses. Overzealous immune and inflammatory responses occur in various clinical conditions, for examples, allergic and autoimmune diseases, and infectious disease where immune and inflammatory responses to infections cause collateral damages to tissues. Such treatments could also simultaneously suppress tissue cell hyperplasia that often accompanies inflammation.

Further, the present study provides new insights into the role of pH in tumorigenesis. Previous study has found that acidic tumor microenvironment (TME) promotes tumor invasion of local tissue. (*42*). Therefore, it has been believed that acidic environment is favorable for tumorigenesis, and neutralizing the acidic TME by alkaline treatment has been proposed as anti-tumor therapy. (*43*). However, according to the present study, low pH is unfavorable to tumor cell proliferation and could induce apoptosis. Thus, contrary to the previous view, the present study shows that lowering rather than raising pH could be a potentially new anti-tumor therapy by directly inducing

tumor cell apoptosis. Lowering pH could be achieved by inducing accumulation of protons in the tumor cells through over active mitochondrial respiration or inhibiting the export of protons or acids to the extracellular space or the import of bicarbonate or other alkaline substances to the cells. Alternatively, lowering pH could be achieved by exogenous reduction of pH in tumor extracellular space, for example by acid treatment as in this study, that over powers the tumor cells' ability to maintain high intracellular pH. Since small molecular pH modifiers such as acids can permeate all tissues, they could be particularly anti-tumor agents at the early or metastatic phases of tumorigenesis when the tumor cells are difficult to locate. In contrast, the present study shows that alkaline treatment carries an inherent risk of increasing tumor cell proliferation, nonetheless, patients could benefit from its enhancement of proliferation of anti-tumor lymphocytes or other inflammatory cells.

A related aspect of the findings in the present study is that different cells varied in their responses to pH modifiers. For example, B cells in the MLNs were less susceptible to acid-induced depletion than T cells. The exact mechanisms for the difference is unknown, but could be attributable to their different expression and/or activities of the enzymes and membrane transporters responsible for pH homeostasis, or different anatomical distribution in the lymph nodes. In addition, different pH modifiers of the same class could have varied effects on the same cells. For example, HOAc was found to have stronger effects than HCl in inducing lymphocyte death in the MLNs. Furthermore, the stronger effects of in vitro treatments than in vivo treatments showed that the concentration or dose of pH modifiers and the duration of treatment are also important factors that determine the effects of pH modifiers. These features can be exploited to

selectively target pathological cells or protective normal cells for the treatment and prevention of diseases such as inflammatory, neoplastic and infectious diseases where cell proliferation contributes to pathogenesis. Thus, by selecting pH modifiers, their doses and dosing regimens, it is possible to achieve selective inhibition and stimulation of pathological cells and protective normal cells, respectively. Such strategy may also be applied to vaccine design to enhance or shape the types of immune responses to the vaccines by selectively promoting or suppressing certain lymphocyte subsets.

As indicated by the foregoing discussion, it should be pointed out that pH modifiers for disease treatment and prevention should include not only acids, bases and pH buffering agents, but also ionophores, and inhibitors and stimulators of the expression and activities of enzymes (e.g., carbonic anhydrases), membrane transporters (e.g., monocarboxylate transporters, Na^+/H^+ exchangers) and ion channels that that are responsible for the maintenance and change of pH in and around a cell.

Finally, although it is generally believed that the pH in a human or animal is maintained at a stable level of about 7.45, humans can experience transient severe acidosis without serious pathological consequences in the aftermath. (*44-46*). In the present study, local administration of pH modifiers in the lungs or abdomen was well tolerated by the animals. Therefore, disease treatments and prevention with pH modifiers can be reasonably expected to be well tolerated by human and animal subjects.

Materials and Methods

CFSE labeling and activation of lymph node cells

Lymph node cells were washed 3 times with plain PBS. After the wash, the cells (3-5 x 10^6/ml) were incubated in 1μm Carboxyfluorescein succinimidyl ester (CFSE) (Fluka/Sigma-Aldrich, Burlington, VT) in plain PBS at room temperature for 7 minutes. After the incubation, 1/4 volume of FBS was added to stop the labeling, and cells were washed 4 times with PBS plus 1% FBS. The labeled cells were cultured with IL-2 (20 units/ml) or IL-2 plus anti-CD3 antibody (1μg/ml) (BD Pharmingen (San Diego, CA). Alternatively, the labeled cells were cultured with IL-4 (4ng/ml) or IL-4 plus lipopolysaccharide (LPS) (10μg/ml) (Sigma-Aldrich, St. Louis, MO). Two and half days later, cells were harvested for further experiments.

Measuring intracellular pH

Intracelluar pH of the CFSE labeled and active cells was measured using the Intracellular pH detection pack according to the manufacture's instruction. (ThermoFisher Scientific, Waltham, MA). containing the pH indicators pHrodo™ Green AM sd and the PowerLoad was purchased from ThermoFisher Scientific (Waltham, MA). Briefly, cells were washed once with Live Cell Image Solution (LCIS) (Life Technoology/ThermoFisher Scientific, Grand Island, NY). Immediately prior to use, the pH indicator pHrodo™ Red AM and the PowerLoad were mixed then diluted in the LCIS to produce working solution containing 0.5-1μM pH indicator. The cells (1-2 x 10^7/ml) were suspended in the working solution and incubated in a 37°C water bath for 30 minutes. After the incubation, the cells were washed once in LCIS containing 1% FBS, and stained with Zombie-Violet viability dye. (Biolegend, San Diego, CA). Fluorescence emitted by the pH indicators was detected by flow cytometry.

OVA sensitization, challenge and treatments of mice

Animal studies were performed according to the protocols approved by the Charles River Accelerator and Development Lab (CRADL) (Cambridge, MA, USA) Institutional Animal Care and Use Committee (IACUC), and essentially as previously described. (*47, 48*). Briefly, Balb/c mice were sensitized by i.p. injection of 20μg OVA (Sigma-Aldrich, St. Louis, MO) plus Alum adjuvant (Thermo Scientific, Rockford, IL). Two weeks later, the sensitization is repeated with 500μg OVA. About 2.5 weeks later, mice were challenged with 100μg OVA in saline by intratracheal instillation, and challenges were repeated as described in each experiment. For acid treatments, 60μl saline containing 175mM HOAc or HCl alone with OVA challenge. Since mice were less tolerant to NaOH by intratracheal instillation, NaOH treatments were carried out by i.p. injection of 200μl of saline containing 87.5mM NaOH. After the challenge and treatment, mediatinal lymph nodes were collected at the times specified in the different experiments.

In vitro treatments of lymphocytes and tumor cells

Lymph node cells (4 x 10^6 cells/ml) were incubated in FBS containing 10% of saline or 87.5mM HCl, HOAc or NaOH prepared in saline in 37°C water bath for 5 hours before analyses. The Jurkat and Raji cells (2 x 10^6 cells/ml) were incubated in FBS containing 10% saline or 87.5mM HCl, HOAc or NaOH prepared in saline in 37°C water bath for 3-5 hours.

Flow cytometry

Fluorochrome-conjugated anti-mouse antibodies against CD4, CD8, CD19 and Ki-67 (PE), Zombie-Green and Zombie-Violet fixable viability dyes and Foxp3 buffer set were purchased from Biolegend (San Diego, CA). Lymphocytes were first stained with

Zombie viability dye, followed by staining for cell surface marker CD4, CD8 and CD19. The cells were then fixed with CytoFix/CytoPerm buffer, washed with PBS plus 1% FBS and 1x CytoPerm buffer, and stained for Ki-67. Human Jurkat cells were stained with Zombie dye followed by fixation, permealization and staining with anti-human Ki-67 (PE). (Biolegend, San Diego, CA). For apoptosis assay, cells were washed twice with plain PBS and once with Annexin V binging buffer (10mM HEPES, pH7.4, 140mM NaCl, 2.5mM $CaCl_2$) and incubated with fluorochrome-conjugated Annexin V in Annexin V binding buffer for 15min at room temperature. The cells were washed twice in Annexin V binding buffer, and resuspended in Annexin V binding buffer. 7-AAD was added to the cells before analyzed by flow cytometry.

References

1. M. Adachi, R. Watanabe-Fukunaga, S. Nagata, Aberrant transcription caused by the insertion of an early transposable element in an intron of the Fas antigen gene of lpr mice. *Proc Natl Acad Sci U S A* **90**, 1756-1760 (1993).
2. F. Burnet, *The Clonal Selection Theory of Acquired Immunity*. (Cambridge University Press, London, 1959).
3. D. A. Hildeman, Y. Zhu, T. C. Mitchell, J. Kappler, P. Marrack, Molecular mechanisms of activated T cell death in vivo. *Curr Opin Immunol* **14**, 354-359 (2002).
4. X. Liu, C. N. Kim, J. Yang, R. Jemmerson, X. Wang, Induction of apoptotic program in cell-free extracts: requirement for dATP and cytochrome c. *Cell* **86**, 147-157 (1996).

5. P. E. Czabotar, G. Lessene, A. Strasser, J. M. Adams, Control of apoptosis by the BCL-2 protein family: implications for physiology and therapy. *Nat Rev Mol Cell Biol* **15**, 49-63 (2014).

6. P. J. Jost *et al.*, XIAP discriminates between type I and type II FAS-induced apoptosis. *Nature* **460**, 1035-1039 (2009).

7. H. Li, H. Zhu, C. J. Xu, J. Yuan, Cleavage of BID by caspase 8 mediates the mitochondrial damage in the Fas pathway of apoptosis. *Cell* **94**, 491-501 (1998).

8. X. Luo, I. Budihardjo, H. Zou, C. Slaughter, X. Wang, Bid, a Bcl2 interacting protein, mediates cytochrome c release from mitochondria in response to activation of cell surface death receptors. *Cell* **94**, 481-490 (1998).

9. S. H. Friend *et al.*, A human DNA segment with properties of the gene that predisposes to retinoblastoma and osteosarcoma. *Nature* **323**, 643-646 (1986).

10. R. A. Weinberg, The retinoblastoma protein and cell cycle control. *Cell* **81**, 323-330 (1995).

11. T. Akiyama, T. Ohuchi, S. Sumida, K. Matsumoto, K. Toyoshima, Phosphorylation of the retinoblastoma protein by cdk2. *Proc Natl Acad Sci U S A* **89**, 7900-7904 (1992).

12. M. E. Ewen *et al.*, Functional interactions of the retinoblastoma protein with mammalian D-type cyclins. *Cell* **73**, 487-497 (1993).

13. P. W. Hinds *et al.*, Regulation of retinoblastoma protein functions by ectopic expression of human cyclins. *Cell* **70**, 993-1006 (1992).

14. J. Kato, H. Matsushime, S. W. Hiebert, M. E. Ewen, C. J. Sherr, Direct binding of cyclin D to the retinoblastoma gene product (pRb) and pRb phosphorylation by the cyclin D-dependent kinase CDK4. *Genes Dev* **7**, 331-342 (1993).

15. S. P. Chellappan, S. Hiebert, M. Mudryj, J. M. Horowitz, J. R. Nevins, The E2F transcription factor is a cellular target for the RB protein. *Cell* **65**, 1053-1061 (1991).

16. N. Dyson *et al.*, Analysis of p107-associated proteins: p107 associates with a form of E2F that differs from pRB-associated E2F-1. *J Virol* **67**, 7641-7647 (1993).

17. O. Warburg, Versuche an überlebendem Carcinomgewebe. *Biochem Zschr* **142**, 317–333 (1923).

18. O. Warburg, On the origin of cancer cells. *Science* **123**, 309-314 (1956).

19. I. Martinez-Reyes, N. S. Chandel, Cancer metabolism: looking forward. *Nat Rev Cancer* **21**, 669-680 (2021).

20. M. G. Vander Heiden, L. C. Cantley, C. B. Thompson, Understanding the Warburg effect: the metabolic requirements of cell proliferation. *Science* **324**, 1029-1033 (2009).

21. P. Vaupel, G. Multhoff, The Warburg Effect: Historical Dogma Versus Current Rationale. *Adv Exp Med Biol* **1269**, 169-177 (2021).

22. L. Stryer, *Biochemistry*. (W. H. Freeman and Company, New York – Basingstoke, ed. 4th, 1995).

23. M. Potter, E. Newport, K. J. Morten, The Warburg effect: 80 years on. *Biochem Soc Trans* **44**, 1499-1505 (2016).

24. G. Grasmann, E. Smolle, H. Olschewski, K. Leithner, Gluconeogenesis in cancer cells - Repurposing of a starvation-induced metabolic pathway? *Biochim Biophys Acta Rev Cancer* **1872**, 24-36 (2019).

25. Z. Darzynkiewicz *et al.*, Initiation and termination of DNA replication during S phase in relation to cyclins D1, E and A, p21WAF1, Cdt1 and the p12 subunit of DNA polymerase delta revealed in individual cells by cytometry. *Oncotarget* **6**, 11735-11750 (2015).

26. I. Vermes, C. Haanen, H. Steffens-Nakken, C. Reutelingsperger, A novel assay for apoptosis. Flow cytometric detection of phosphatidylserine expression on early apoptotic cells using fluorescein labelled Annexin V. *J Immunol Methods* **184**, 39-51 (1995).

27. S. Nagata, Apoptosis and Clearance of Apoptotic Cells. *Annu Rev Immunol* **36**, 489-517 (2018).

28. N. U. Meldrum, F. J. Roughton, Carbonic anhydrase. Its preparation and properties. *J Physiol* **80**, 113-142 (1933).

29. B. C. Tripp, K. Smith, J. G. Ferry, Carbonic anhydrase: new insights for an ancient enzyme. *J Biol Chem* **276**, 48615-48618 (2001).

30. V. R. Fantin, J. St-Pierre, P. Leder, Attenuation of LDH-A expression uncovers a link between glycolysis, mitochondrial physiology, and tumor maintenance. *Cancer Cell* **9**, 425-434 (2006).

31. D. F. Rolfe, G. C. Brown, Cellular energy utilization and molecular origin of standard metabolic rate in mammals. *Physiol Rev* **77**, 731-758 (1997).

32. S. E. LeBoeuf *et al.*, Activation of Oxidative Stress Response in Cancer Generates a Druggable Dependency on Exogenous Non-essential Amino Acids. *Cell Metab* **31**, 339-350 e334 (2020).

33. N. N. Pavlova, C. B. Thompson, The Emerging Hallmarks of Cancer Metabolism. *Cell Metab* **23**, 27-47 (2016).

34. T. Pfeiffer, A. Morley, An evolutionary perspective on the Crabtree effect. *Front Mol Biosci* **1**, 17 (2014).

35. N. Ziv, N. J. Brandt, D. Gresham, The use of chemostats in microbial systems biology. *J Vis Exp*, (2013).

36. A. Flamholz, E. Noor, A. Bar-Even, W. Liebermeister, R. Milo, Glycolytic strategy as a tradeoff between energy yield and protein cost. *Proc Natl Acad Sci U S A* **110**, 10039-10044 (2013).

37. G. N. Vemuri, E. Altman, D. P. Sangurdekar, A. B. Khodursky, M. A. Eiteman, Overflow metabolism in Escherichia coli during steady-state growth: transcriptional regulation and effect of the redox ratio. *Appl Environ Microbiol* **72**, 3653-3661 (2006).

38. C. A. Homewood, Carbohydrate metabolism of malarial parasites. *Bull World Health Organ* **55**, 229-235 (1977).

39. J. Moyersoen, J. Choe, E. Fan, W. G. Hol, P. A. Michels, Biogenesis of peroxisomes and glycosomes: trypanosomatid glycosome assembly is a promising new drug target. *FEMS Microbiol Rev* **28**, 603-643 (2004).

40. H. You, R. J. Stephenson, G. N. Gobert, D. P. McManus, Revisiting glucose uptake and metabolism in schistosomes: new molecular insights for improved schistosomiasis therapies. *Front Genet* **5**, 176 (2014).

41. Q. Wu *et al.*, Systematic review and meta-analysis of the epidemiology of vancomycin-resistance Staphylococcus aureus isolates. *Antimicrob Resist Infect Control* **10**, 101 (2021).

42. V. Estrella *et al.*, Acidity generated by the tumor microenvironment drives local invasion. *Cancer Res* **73**, 1524-1535 (2013).

43. C. Corbet, O. Feron, Tumour acidosis: from the passenger to the driver's seat. *Nat Rev Cancer* **17**, 577-593 (2017).

44. J. Bangsbo, L. Johansen, T. Graham, B. Saltin, Lactate and H+ effluxes from human skeletal muscles during intense, dynamic exercise. *J Physiol* **462**, 115-133 (1993).

45. E. Hopkins, S. Sharma, in *Physiology*. (StatPearls Publishing, NCBI Bookshelf, 2019).

46. C. E. Orringer, J. C. Eustace, C. D. Wunsch, L. B. Gardner, Natural history of lactic acidosis after grand-mal seizures. A model for the study of an anion-gap acidosis not associated with hyperkalemia. *N Engl J Med* **297**, 796-799 (1977).

47. T. Rangasamy *et al.*, Disruption of Nrf2 enhances susceptibility to severe airway inflammation and asthma in mice. *J Exp Med* **202**, 47-59 (2005).

48. W. P. Zeng *et al.*, Staphylococcal enterotoxin A-activated regulatory T cells promote allergen-specific TH2 response to intratracheal allergen inoculation. *J Allergy Clin Immunol* **139**, 508-518 e504 (2017).

Acknowledgments

WZ thanks Dr. Tiru Rangasamy for technical information regarding the mouse asthma model**.**

Author Contribution

WZ conceived, designed and carried out the study, and wrote the manuscript.

Competing interest

WZ is the inventor of a patent application based in part on some data presented in this article.

Data and materials availability

All data are available in the manuscript.

Figure Legends

Figure 1. Positive correlation between intracellular pH and lymphocyte proliferation. CFSE-labeled total lymph node cells were cultured (a) with IL-2 only (left panels), or IL-2 and anti-CD3 antibodies; or (b) with IL-4 or IL-4 and LPS. The cultured cells were sequentially stained with the intracellular pH indicator pHrodo™ Red and Zombie-violet. Flow cytometric pseudocolor plots of CFSE and pHrodo™ Red staining (upper panels) and histograms of CFSE staining of Zombie-violet^{-} live lymphocytes are shown.

Figure 2. Total cell numbers of MLNs. The top panels in (a) and (b) are is a schematics illustrating the schedules for OVA challenges and treatments with saline, or saline plus HCl, or HOAc of OVA-sensitized mice for the first (a) and second (b) sets of experiments. Arrows indicate the time points for the challenges or treatments. Lower panels are graphs showing the average total numbers of MLN cells of mice in the different treatment groups in the first (a) and second (b) set of experiments. Data were pooled from 3 experiments. Statistical significance between saline and the other groups were determined by Student t test; * $p < 0.05$, ** $p < 0.01$.

Figure 3. Lymphocyte populations and proliferation in the MLNs. (a and c) Lymphocyte populations in the MLNs of representative mice of the different treatment groups in the first (a) and second (c) sets of experiments. Top left panels are the same schedules for the challenges and treatments of the mice as in Figure 2. The top right panels are flow cytometry pseudocolor plots showing the gates of two lymphocyte populations (Lym1 and Lym2). Lower panels are pseudocolor plots showing CD4 T cells (Q3), CD8 T cells (Q1) and B cells ($CD19^{+}$) (Q5) in Lym1 (left) and Lym2 (right). Numbers in the plots are the percentages of each cell populations. (b and d) Ki-67 expression in the different lymphocyte populations in the representative mice of the different treatment groups in the first (b) and second (d) sets of experiments. Left panels are histograms showing the expression of Ki-67 in Lym1 and Lym2 and their respective B cell populations. Numbers are the percentages of Ki-67 high, low or negative cells. Right panels are graphic presentation of the percentages of Ki-67^{hi} and Ki-67^{lo} cells shown in the histograms. (e) Graph showing the mean fluorescence intensities of Ki-67^{hi}

cells in the Lym2 populations and its B cells of the different treatment groups in the second set of experiments.

Figure 4. Ki-67 expression by different lymphocyte populations of lymph node cells treated in vitro. Primary lymph node cells were incubated in FBS containing 10% saline or saline containing HCl, HOAc or NaOH. Live cells were analyzed by flow cytometry determine Ki-67 expression in total lymphocytes, CD4, CD8 T cells and B cells ($CD19^+$). Left panels are histograms of Ki-67 staining. Numbers in the histograms are percentages of Ki-67^+ cells in the different lymphocyte populations. Right panel is graphic presentation of the percentages of Ki-67^+ cells in the different lymphocyte populations shown in the histograms.

Figure 5. Correlation between low pH and lymphocyte apoptosis. Shown are peripheral lymphocytes derived from unimmunized mice (a, b), in vitro cultures with anti-CD3 plus IL-2 (c, d) or LPS plus IL-4 (e, f) treated with saline or saline containing HOAc or NaOH, MLNs of mice sensitized and challenged with OVA and treated in vivo with saline or saline containing HOAc or NaOH in FBS (g, h), or MLN cells from OVA sensitized and challenged but untreated mice that were treated in vitro with saline or saline containing HOAc or NaOH in FBS (j, k). The cells were stained with intracellular pH indicator pHrodo™ Green, Annexin V, and 7-AAD or Zombie-violet. Pseudocolor plots of Annexin V and 7-AAD or Zombie-violet staining of total lymphocytes or gated B cells, CD4 T and CD8 T cells (a, c, e, g, j), or pHrodo™ Green and Annexin V staining of gated live total lymphocytes, B cells, CD4 and CD8 T cells (b, d, f, h, k) are shown. Bar graphs (i) show the mean fluorescence intensities (MFI) of pHrodo™ Green of the early

apoptotic Annexin V^{high} cells (Q1) and the non-apoptotic Annexin V^{low} cells (Q4) in the pH high populations of the ex vivo MLN cells in (h).

Figure 6. Effects of pH modifiers on viability and Ki-67 expression of tumor cells. (a) Comparison of average viabilities of Jurkat and Raji cells by Tryplan Blue staining in the different treatment groups as indicated. Statistical significance of differences between saline and other treatment groups was determined by Student t test, * $p < 0.05$, ** $p < 0.01$. (b) Histograms of Ki-67 staining in live (Zombie negative) Jurkat or Raji cells after the different treatments as indicated. The numbers in the histograms are the percentages of Ki-67^{+} Jurkat cells, or Raji cells with high, low or negative expression of Ki-67.

Figure 7. Correlation between low pH and apoptosis of tumor cells. Jurkat (a) and Raji (b) cells were treated with saline or saline containing HOAc or NaOH in FBS. Pseudocolor plots of staining of Annexin V and 7-AAD of total tumor cells (upper panels), or staining of Annexin V and pHrodo™ Green of gated live (7-AAD negative) tumor cells (lower panels) are shown.

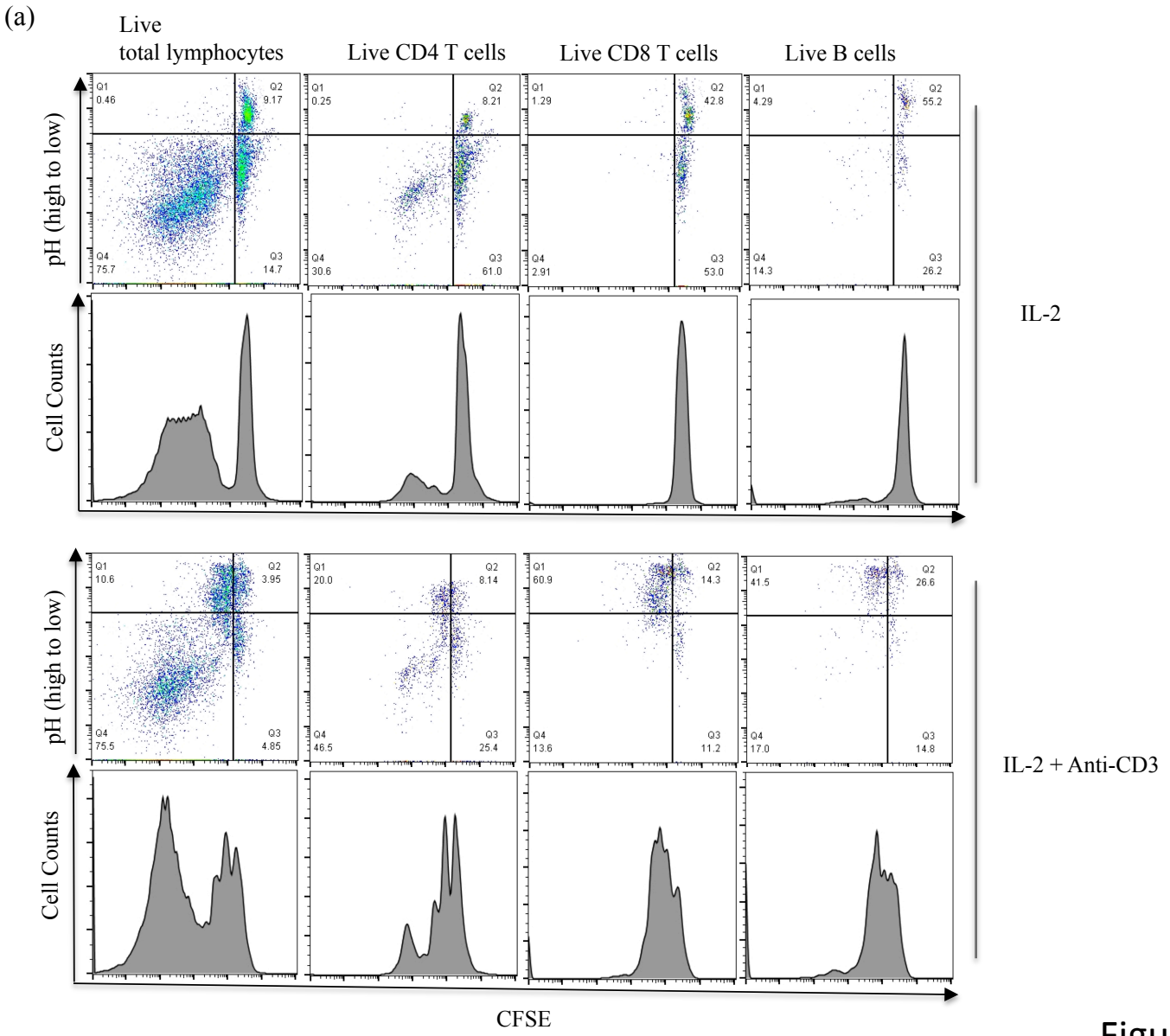
(a)
Live
total lymphocytes
Live CD4 T cells
Live CD8 T cells
Live B cells
pH (high to low)
Cell Counts
Q1 0.46
Q2 9.17
Q4 75.7
Q3 14.7
Q1 0.25
Q2 8.21
Q4 30.6
Q3 61.0
Q1 1.29
Q2 42.8
Q4 2.91
Q3 53.0
Q1 4.29
Q2 55.2
Q4 14.3
Q3 26.2
IL-2
Q1 10.6
Q2 3.95
Q4 75.5
Q3 4.85
Q1 20.0
Q2 8.14
Q4 46.5
Q3 25.4
Q1 60.9
Q2 14.3
Q4 13.6
Q3 11.2
Q1 41.5
Q2 26.6
Q4 17.0
Q3 14.8
IL-2 + Anti-CD3
CFSE

Figure 1a

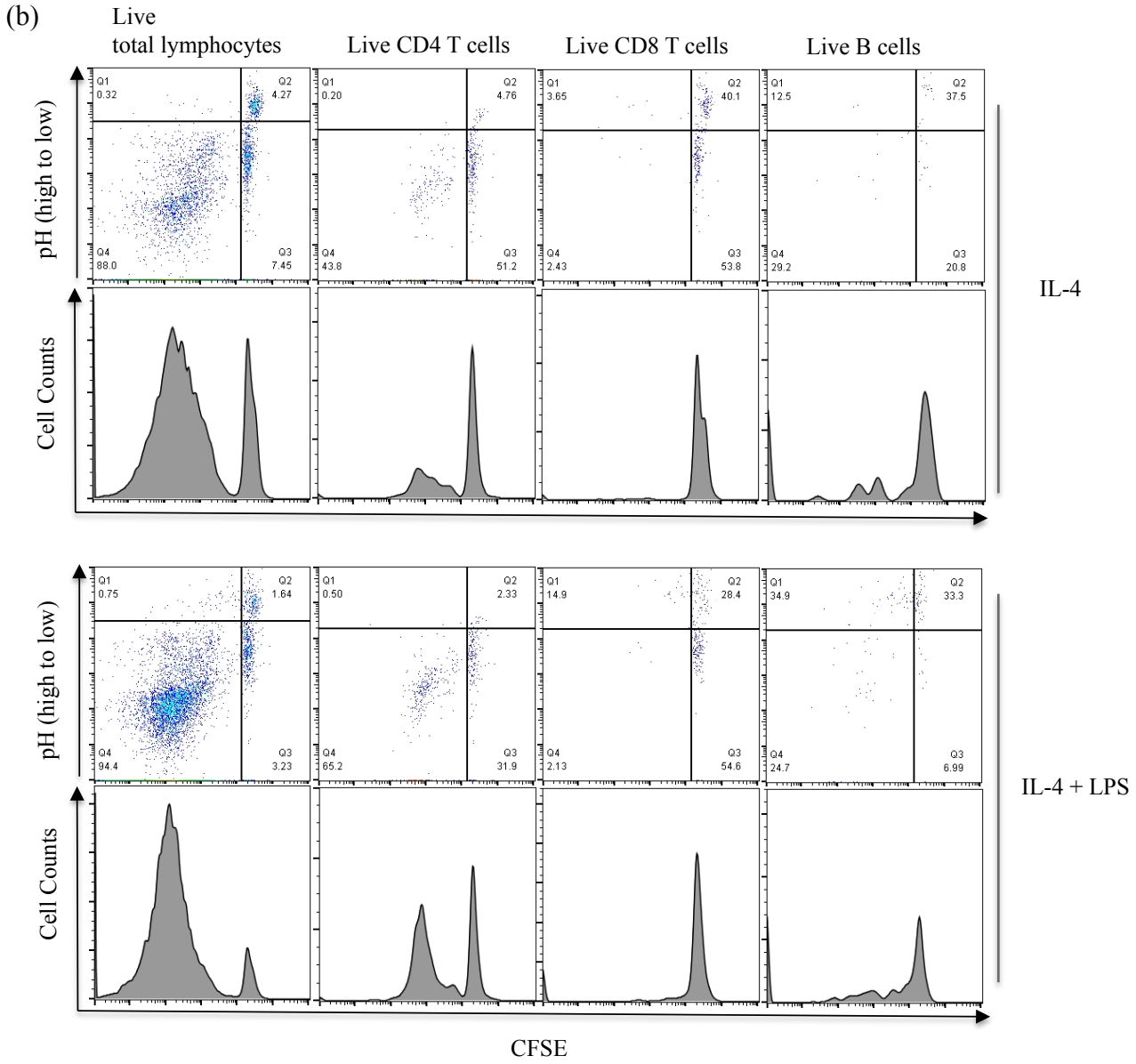
(b)
Live
total lymphocytes
Live CD4 T cells
Live CD8 T cells
Live B cells
pH (high to low)
Cell Counts
Q1 0.32
Q2 4.27
Q4 88.0
Q3 7.45
Q1 0.20
Q2 4.76
Q4 43.8
Q3 51.2
Q1 3.65
Q2 40.1
Q4 2.43
Q3 53.8
Q1 12.5
Q2 37.5
Q4 29.2
Q3 20.8
IL-4
Q1 0.75
Q2 1.64
Q4 94.4
Q3 3.23
Q1 0.50
Q2 2.33
Q4 65.2
Q3 31.9
Q1 14.9
Q2 28.4
Q4 2.13
Q3 54.6
Q1 34.9
Q2 33.3
Q4 24.7
Q3 6.99
IL-4 + LPS
CFSE

Figure 1b

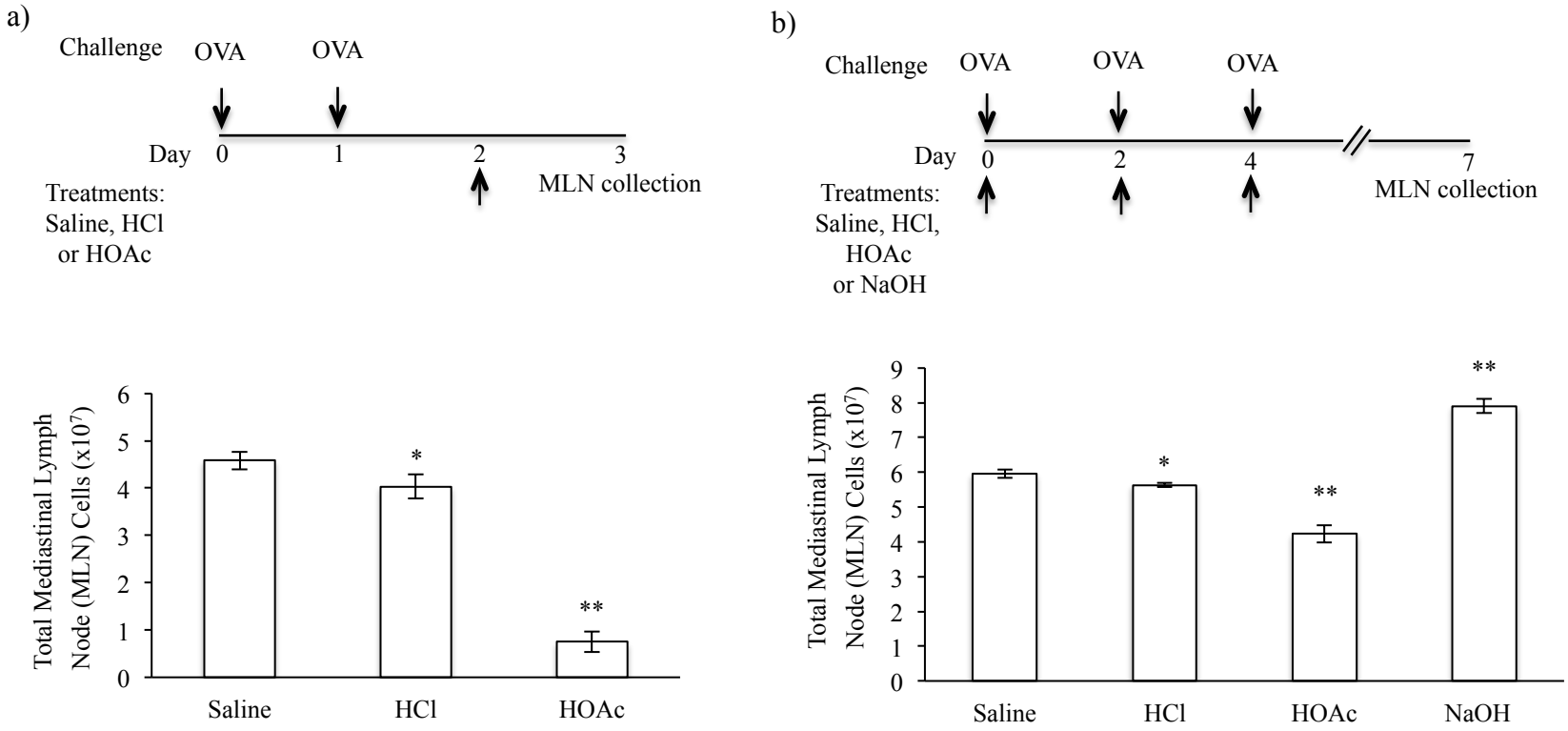
a)
Challenge
OVA
OVA
Day
0
1
2
3
MLN collection
Treatments:
Saline, HCl
or HOAc
Total Mediastinal Lymph
Node (MLN) Cells (x10^7)
6
5
4
3
2
1
0
*
**
Saline
HCl
HOAc
b)
Challenge
OVA
OVA
OVA
Day
0
2
4
7
MLN collection
Treatments:
Saline, HCl,
HOAc
or NaOH
Total Mediastinal Lymph
Node (MLN) Cells (x10^7)
9
8
7
6
5
4
3
2
1
0
*
**
**
Saline
HCl
HOAc
NaOH

Figure 2

a)

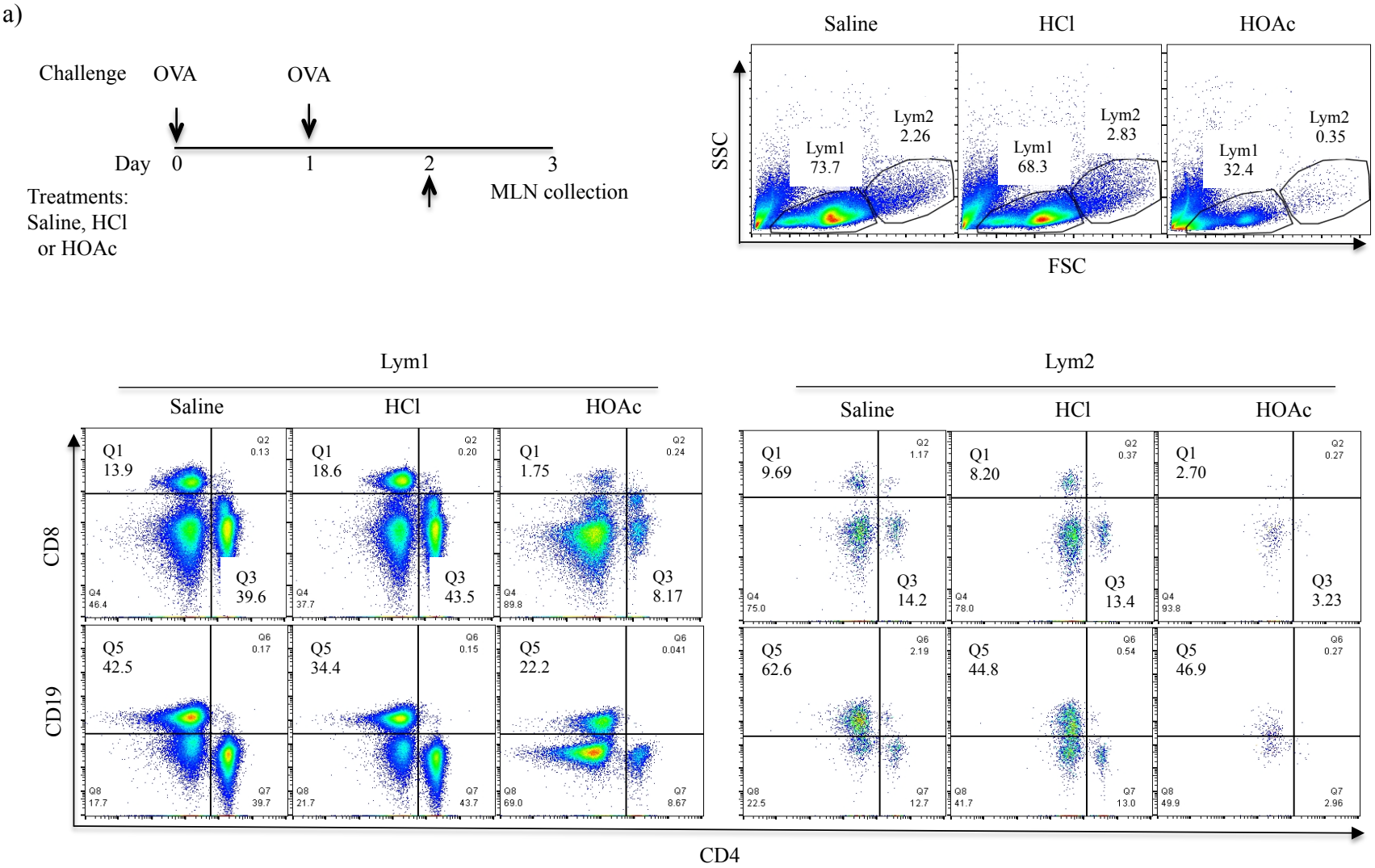
Challenge
OVA
OVA
Day
0
1
2
3
MLN collection
Treatments:
Saline, HCl
or HOAc
Saline
HCl
HOAc
SSC
FSC
Lym1
73.7
Lym2
2.26
Lym1
68.3
Lym2
2.83
Lym1
32.4
Lym2
0.35
Lym1
Lym2
Saline
HCl
HOAc
CD8
CD19
CD4
Q1
13.9
Q2
0.13
Q3
39.6
Q4
46.4
Q5
42.5
Q6
0.17
Q7
39.7
Q8
17.7
Q1
18.6
Q2
0.20
Q3
43.5
Q4
37.7
Q5
34.4
Q6
0.15
Q7
43.7
Q8
21.7
Q1
1.75
Q2
0.24
Q3
8.17
Q4
89.8
Q5
22.2
Q6
0.041
Q7
8.67
Q8
69.0
Q1
9.69
Q2
1.17
Q3
14.2
Q4
75.0
Q5
62.6
Q6
2.19
Q7
12.7
Q8
22.5
Q1
8.20
Q2
0.37
Q3
13.4
Q4
78.0
Q5
44.8
Q6
0.54
Q7
13.0
Q8
41.7
Q1
2.70
Q2
0.27
Q3
3.23
Q4
93.8
Q5
46.9
Q6
0.27
Q7
2.96
Q8
49.9

Figure 3a

b)

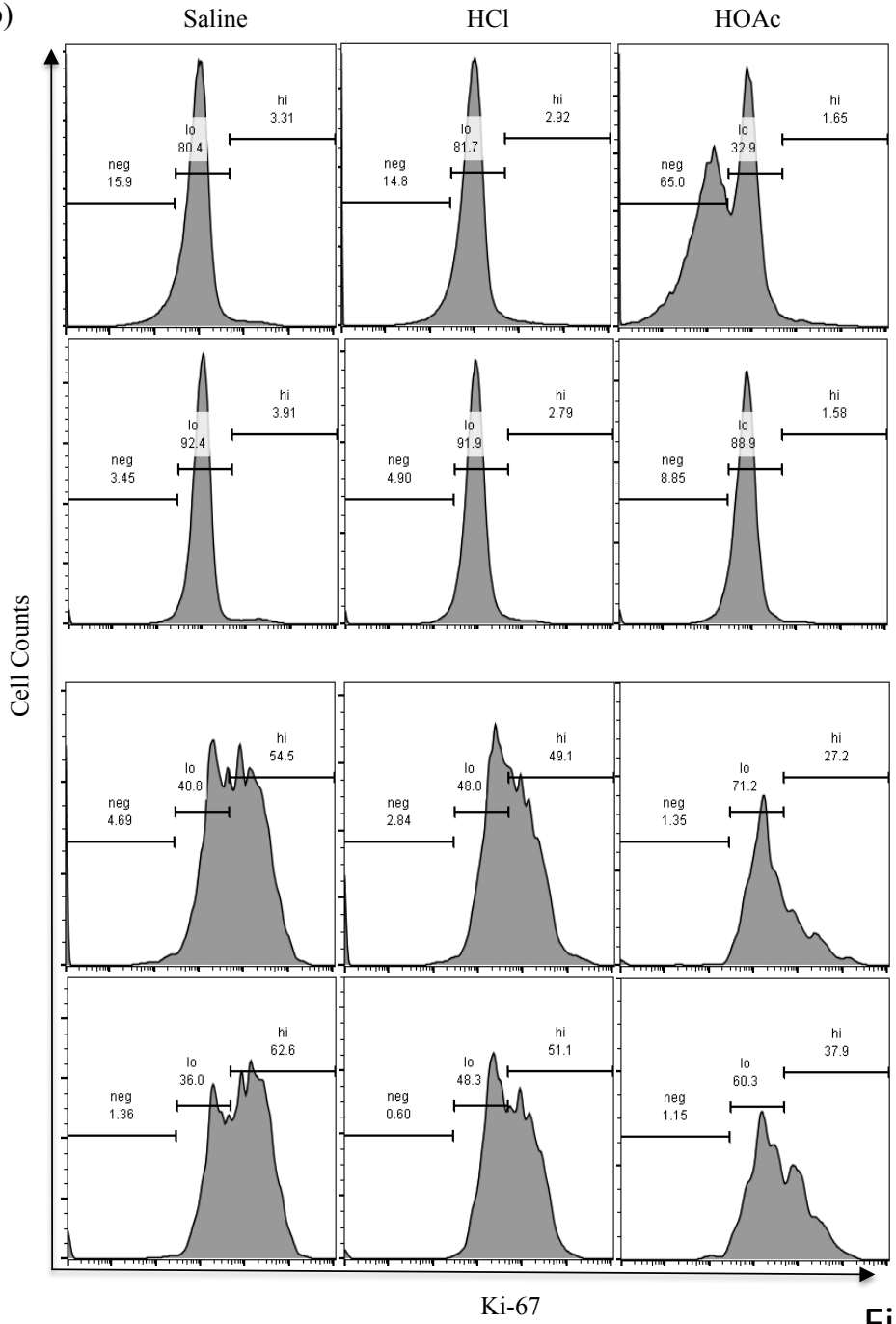
Saline
HCl
HOAc
Cell Counts
Ki-67
neg 15.9
lo 80.4
hi 3.31
neg 14.8
lo 81.7
hi 2.92
neg 65.0
lo 32.9
hi 1.65
neg 3.45
lo 92.4
hi 3.91
neg 4.90
lo 91.9
hi 2.79
neg 8.85
lo 88.9
hi 1.58
neg 4.69
lo 40.8
hi 54.5
neg 2.84
lo 48.0
hi 49.1
neg 1.35
lo 71.2
hi 27.2
neg 1.36
lo 36.0
hi 62.6
neg 0.60
lo 48.3
hi 51.1
neg 1.15
lo 60.3
hi 37.9

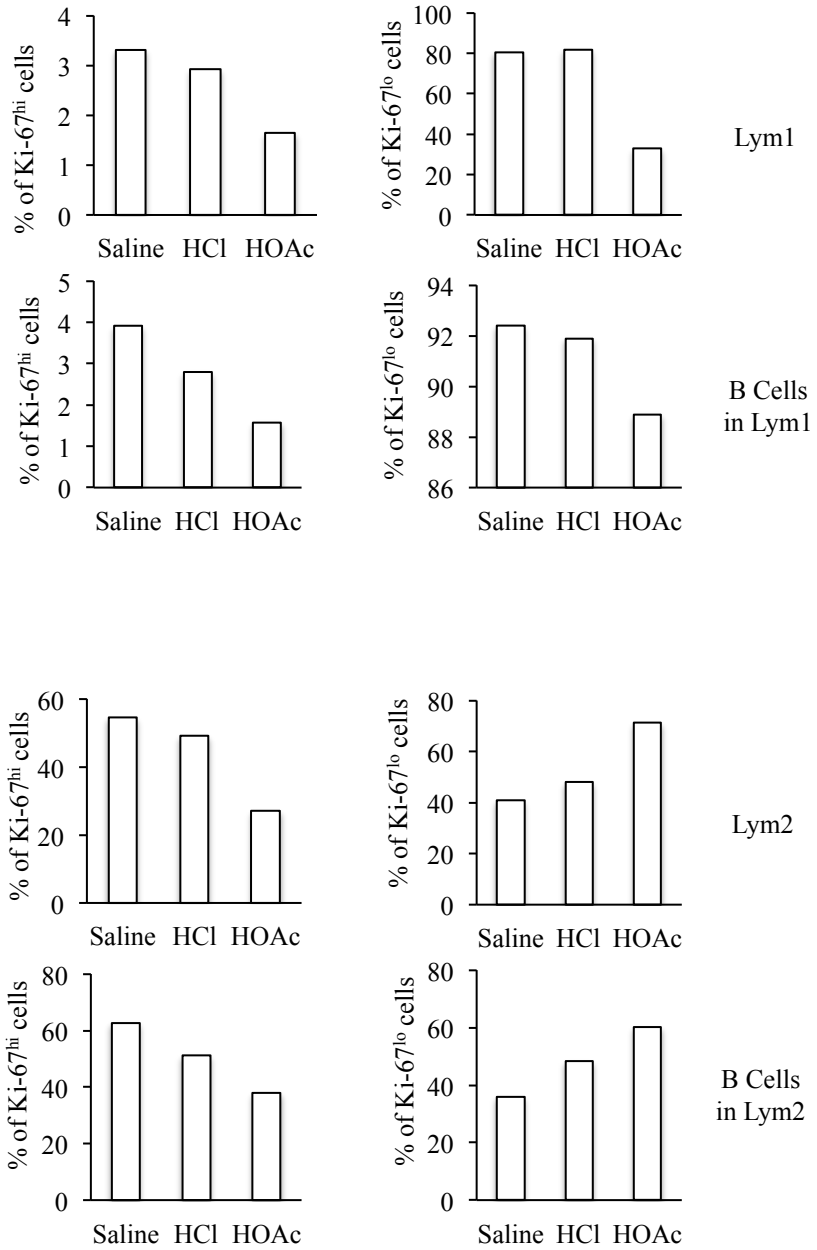
% of Ki-67hi cells
% of Ki-67lo cells
Saline HCl HOAc
Lym1
B Cells in Lym1
Lym2
B Cells in Lym2

Figure 3b

c)

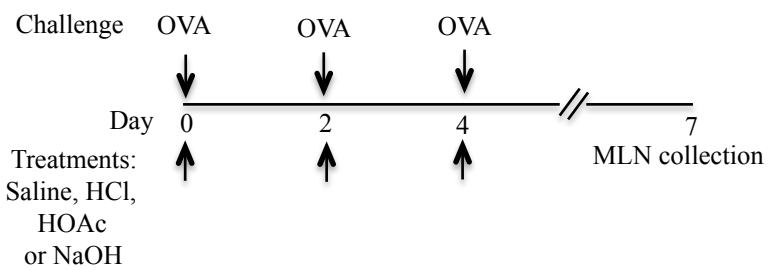
Challenge
OVA
OVA
OVA
Day
0
2
4
7
MLN collection
Treatments:
Saline, HCl,
HOAc
or NaOH

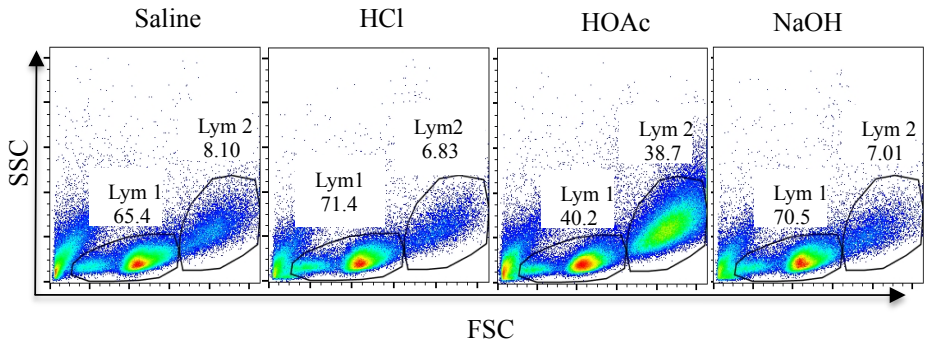
Saline
HCl
HOAc
NaOH
SSC
FSC
Lym 1
65.4
Lym 2
8.10
Lym1
71.4
Lym2
6.83
Lym 1
40.2
Lym 2
38.7
Lym 1
70.5
Lym 2
7.01

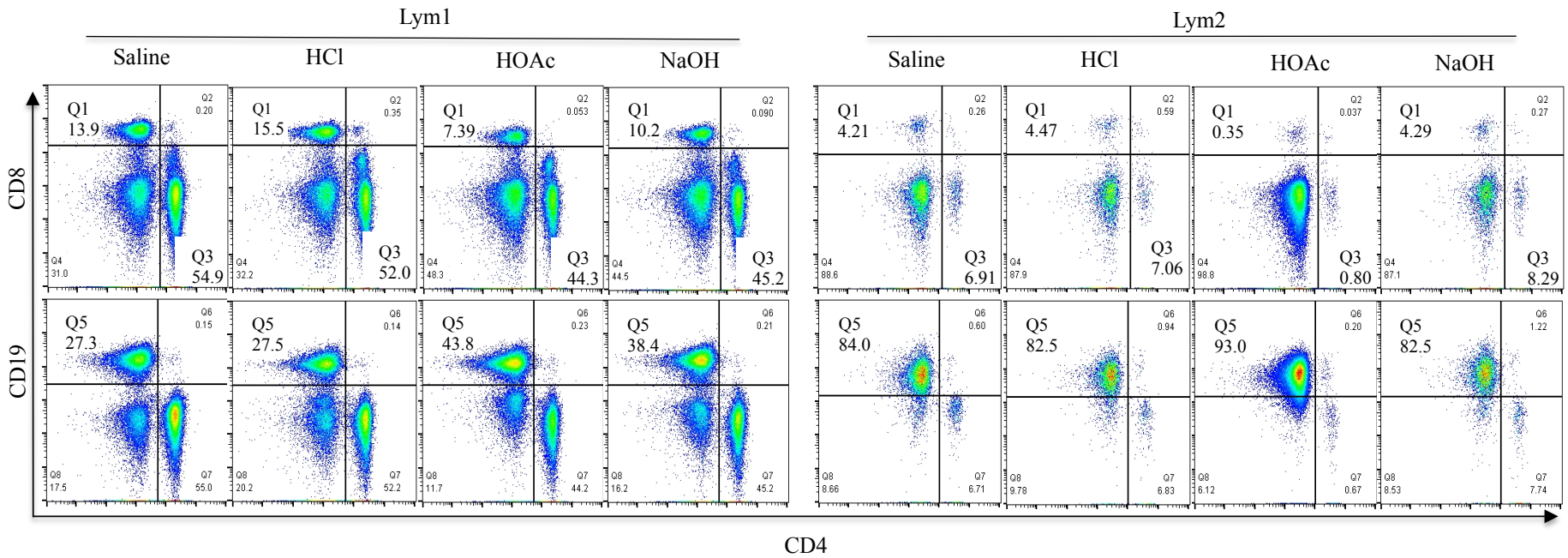
Lym1
Saline
HCl
HOAc
NaOH
Lym2
Saline
HCl
HOAc
NaOH
CD8
CD19
CD4
Q1 13.9
Q2 0.20
Q3 54.9
Q4 31.0
Q5 27.3
Q6 0.15
Q7 55.0
Q8 17.5
Q1 15.5
Q2 0.35
Q3 52.0
Q4 32.2
Q5 27.5
Q6 0.14
Q7 52.2
Q8 20.2
Q1 7.39
Q2 0.053
Q3 44.3
Q4 48.3
Q5 43.8
Q6 0.23
Q7 44.2
Q8 11.7
Q1 10.2
Q2 0.090
Q3 45.2
Q4 44.5
Q5 38.4
Q6 0.21
Q7 45.2
Q8 16.2
Q1 4.21
Q2 0.26
Q3 6.91
Q4 88.6
Q5 84.0
Q6 0.60
Q7 6.71
Q8 8.66
Q1 4.47
Q2 0.59
Q3 7.06
Q4 87.9
Q5 82.5
Q6 0.94
Q7 6.83
Q8 9.78
Q1 0.35
Q2 0.037
Q3 0.80
Q4 98.8
Q5 93.0
Q6 0.20
Q7 0.67
Q8 6.12
Q1 4.29
Q2 0.27
Q3 8.29
Q4 87.1
Q5 82.5
Q6 1.22
Q7 7.74
Q8 8.53

Figure 3c

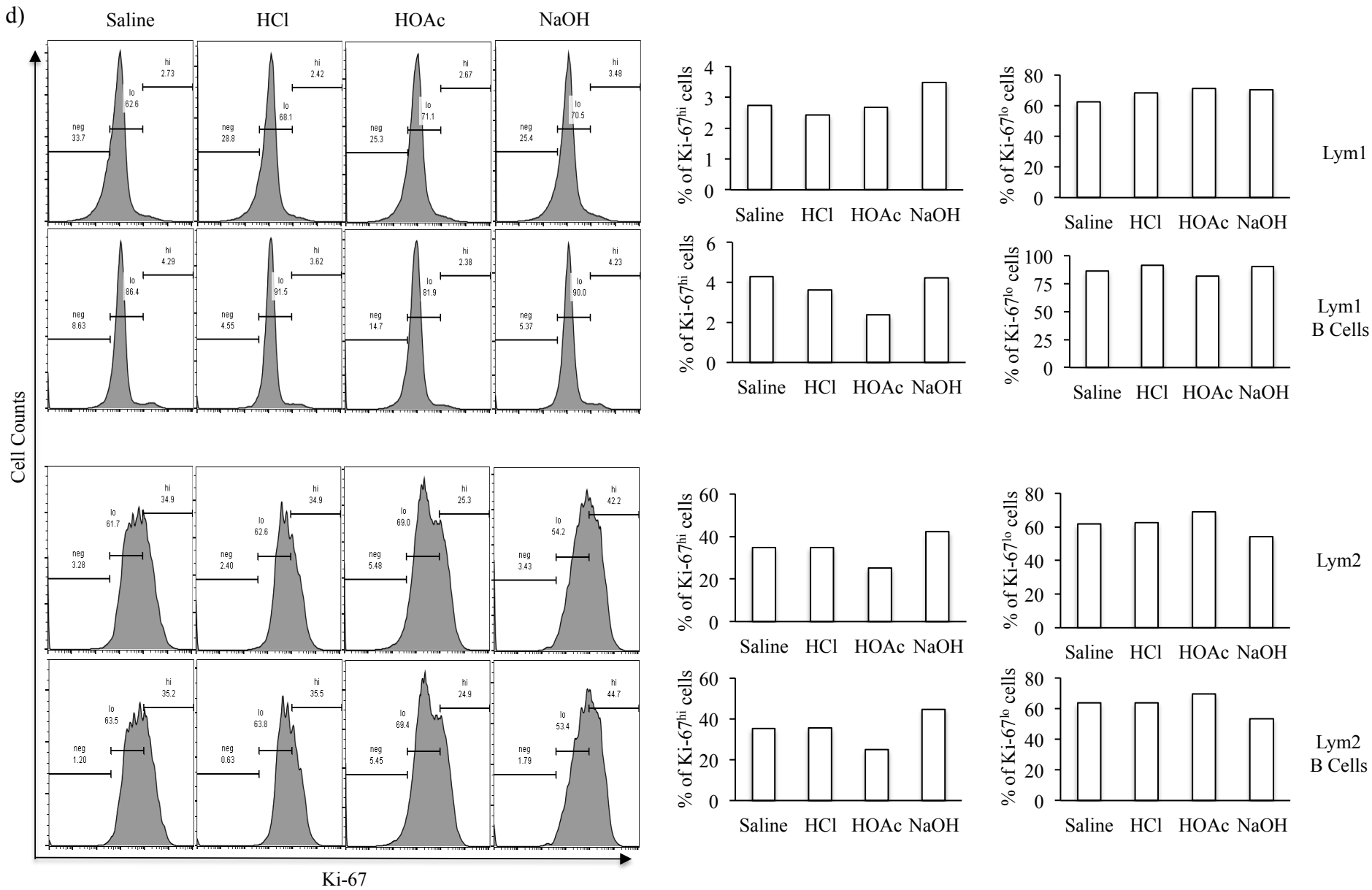
d)
Saline
HCl
HOAc
NaOH
Cell Counts
Ki-67
neg 33.7
lo 62.6
hi 2.73
neg 28.8
lo 68.1
hi 2.42
neg 25.3
lo 71.1
hi 2.67
neg 25.4
lo 70.5
hi 3.48
neg 8.63
lo 86.4
hi 4.29
neg 4.55
lo 91.5
hi 3.62
neg 14.7
lo 81.9
hi 2.38
neg 5.37
lo 90.0
hi 4.23
neg 3.28
lo 61.7
hi 34.9
neg 2.40
lo 62.6
hi 34.9
neg 5.48
lo 69.0
hi 25.3
neg 3.43
lo 54.2
hi 42.2
neg 1.20
lo 63.5
hi 35.2
neg 0.63
lo 63.8
hi 35.5
neg 5.45
lo 69.4
hi 24.9
neg 1.79
lo 53.4
hi 44.7
% of Ki-67hi cells
% of Ki-67lo cells
Lym1
Lym1 B Cells
Lym2
Lym2 B Cells
Saline HCl HOAc NaOH

Figure 3d

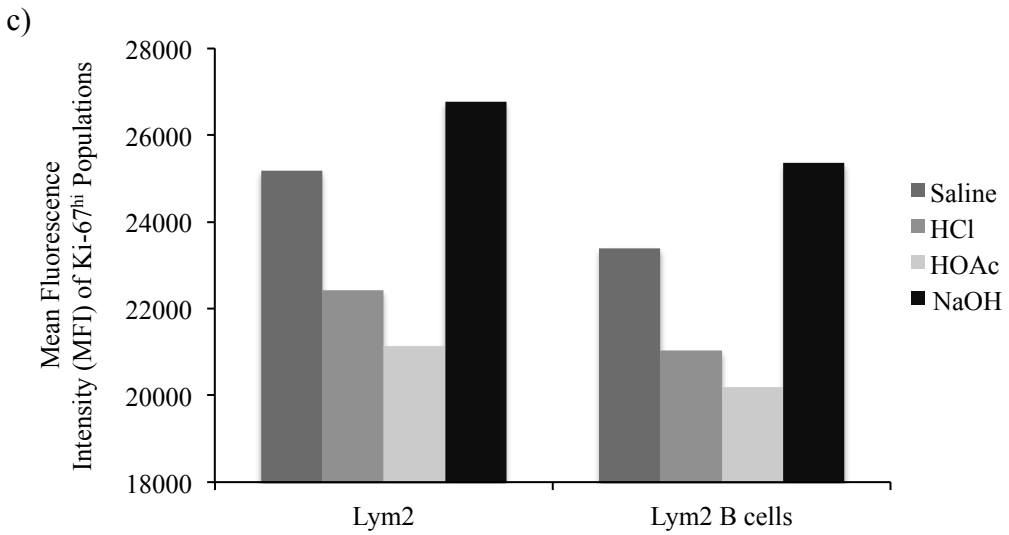
c)
Mean Fluorescence Intensity (MFI) of Ki-67hi Populations
28000
26000
24000
22000
20000
18000
Lym2
Lym2 B cells
Saline
HCl
HOAc
NaOH

Figure 3e

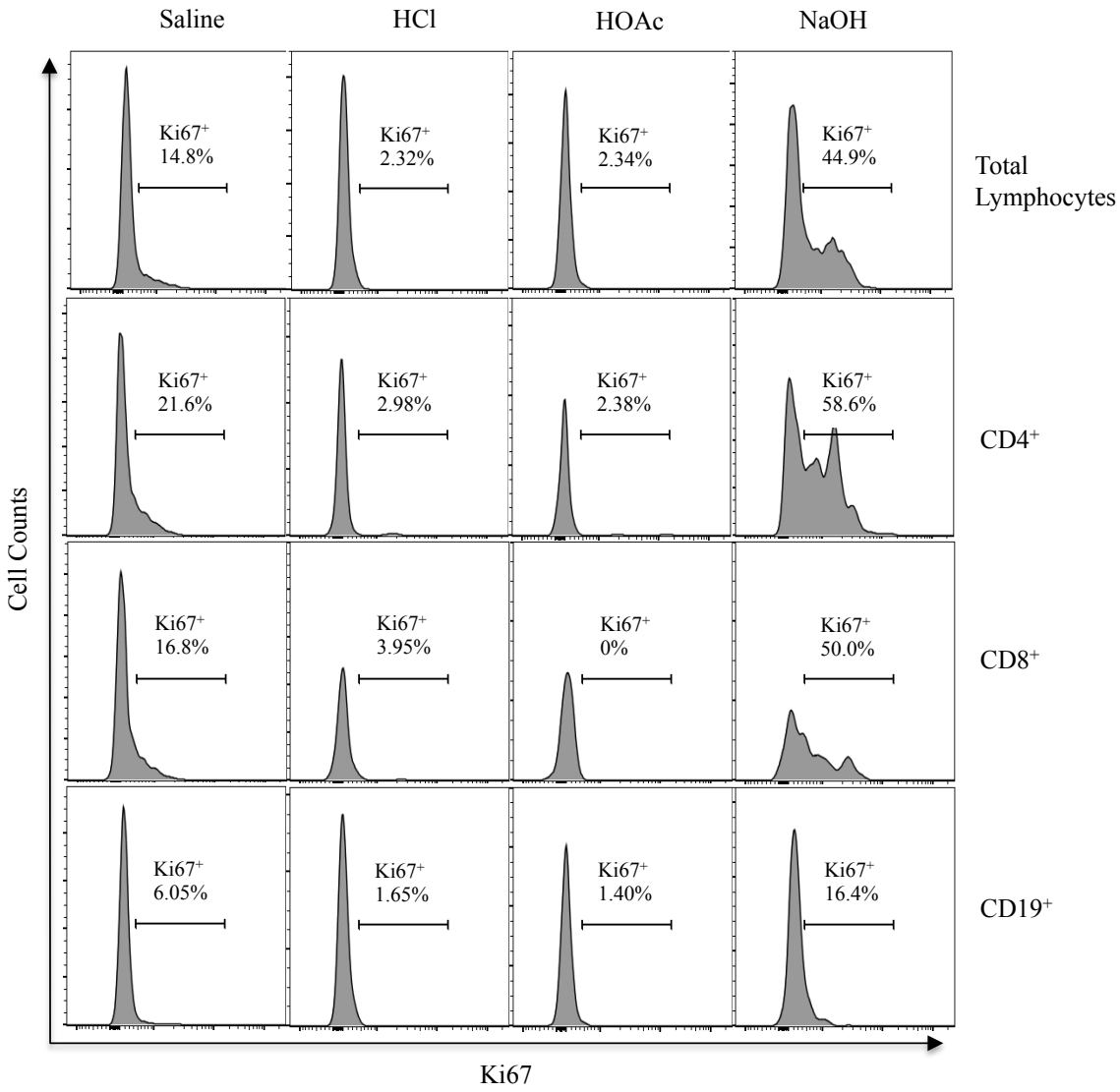
Saline
HCl
HOAc
NaOH
Ki67+ 14.8%
Ki67+ 2.32%
Ki67+ 2.34%
Ki67+ 44.9%
Total Lymphocytes
Ki67+ 21.6%
Ki67+ 2.98%
Ki67+ 2.38%
Ki67+ 58.6%
CD4+
Ki67+ 16.8%
Ki67+ 3.95%
Ki67+ 0%
Ki67+ 50.0%
CD8+
Ki67+ 6.05%
Ki67+ 1.65%
Ki67+ 1.40%
Ki67+ 16.4%
CD19+
Cell Counts
Ki67

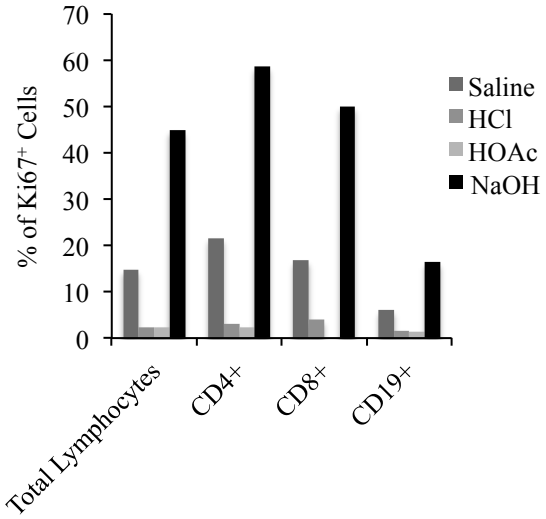
% of Ki67+ Cells
70
60
50
40
30
20
10
0
Saline
HCl
HOAc
NaOH
Total Lymphocytes
CD4+
CD8+
CD19+

Figure 4

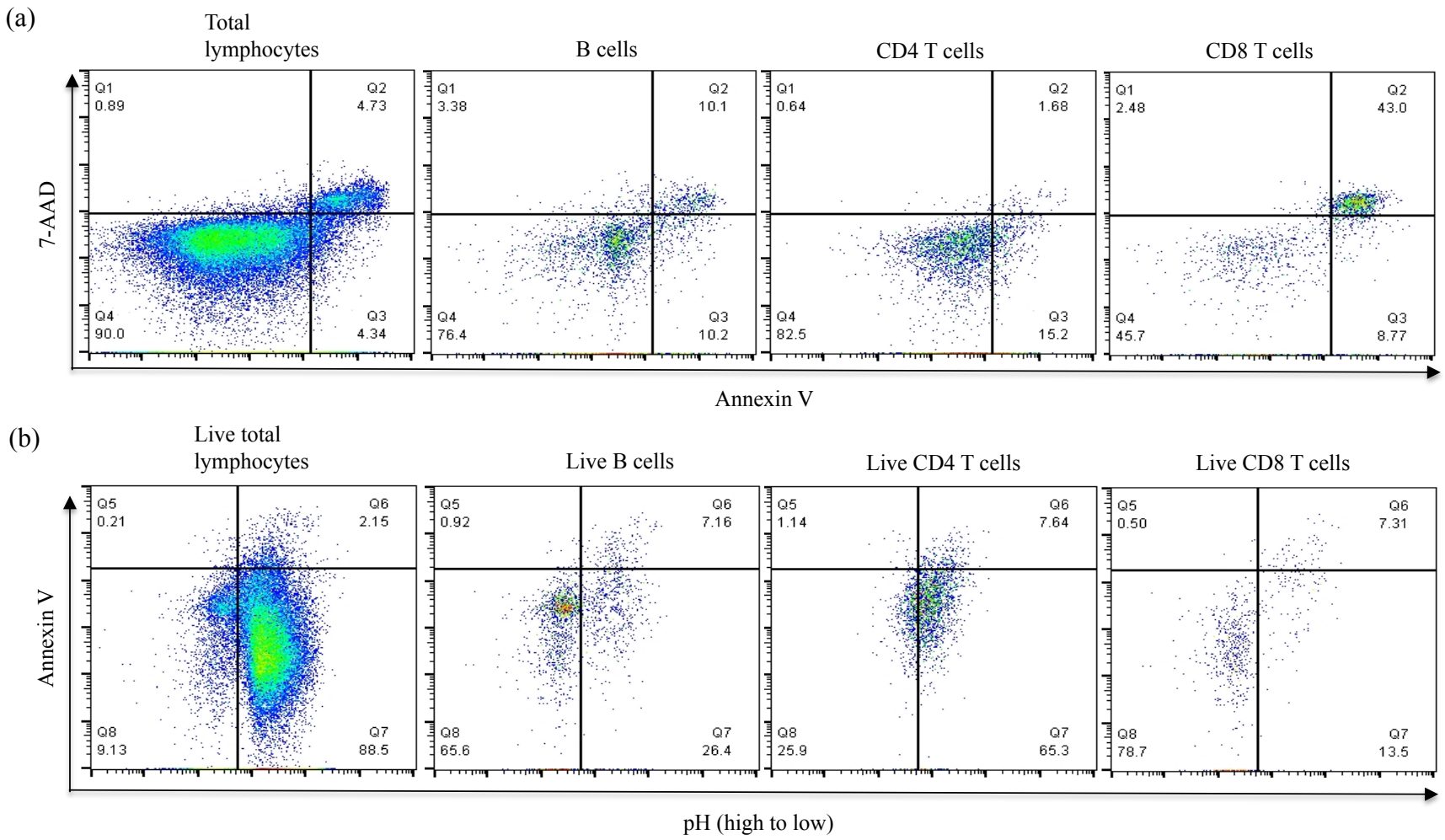
(a)
Total lymphocytes
B cells
CD4 T cells
CD8 T cells
7-AAD
Annexin V
Q1 0.89
Q2 4.73
Q4 90.0
Q3 4.34
Q1 3.38
Q2 10.1
Q4 76.4
Q3 10.2
Q1 0.64
Q2 1.68
Q4 82.5
Q3 15.2
Q1 2.48
Q2 43.0
Q4 45.7
Q3 8.77
(b)
Live total lymphocytes
Live B cells
Live CD4 T cells
Live CD8 T cells
Annexin V
pH (high to low)
Q5 0.21
Q6 2.15
Q8 9.13
Q7 88.5
Q5 0.92
Q6 7.16
Q8 65.6
Q7 26.4
Q5 1.14
Q6 7.64
Q8 25.9
Q7 65.3
Q5 0.50
Q6 7.31
Q8 78.7
Q7 13.5

Figure 5a, b

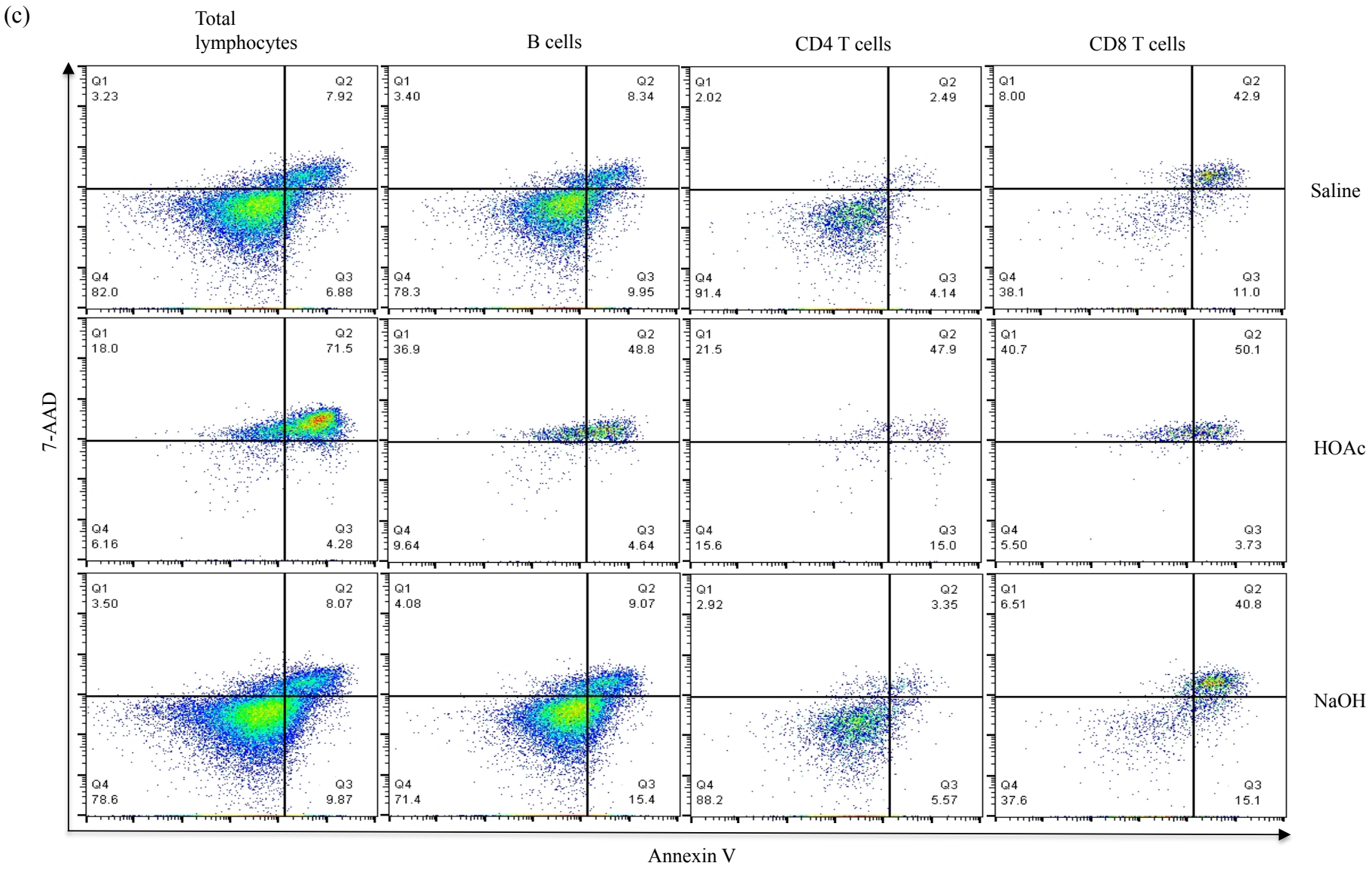
(c)
Total lymphocytes
B cells
CD4 T cells
CD8 T cells
Saline
HOAc
NaOH
7-AAD
Annexin V
Q1 3.23
Q2 7.92
Q4 82.0
Q3 6.88
Q1 3.40
Q2 8.34
Q4 78.3
Q3 9.95
Q1 2.02
Q2 2.49
Q4 91.4
Q3 4.14
Q1 8.00
Q2 42.9
Q4 38.1
Q3 11.0
Q1 18.0
Q2 71.5
Q4 6.16
Q3 4.28
Q1 36.9
Q2 48.8
Q4 9.64
Q3 4.64
Q1 21.5
Q2 47.9
Q4 15.6
Q3 15.0
Q1 40.7
Q2 50.1
Q4 5.50
Q3 3.73
Q1 3.50
Q2 8.07
Q4 78.6
Q3 9.87
Q1 4.08
Q2 9.07
Q4 71.4
Q3 15.4
Q1 2.92
Q2 3.35
Q4 88.2
Q3 5.57
Q1 6.51
Q2 40.8
Q4 37.6
Q3 15.1

Figure 5c

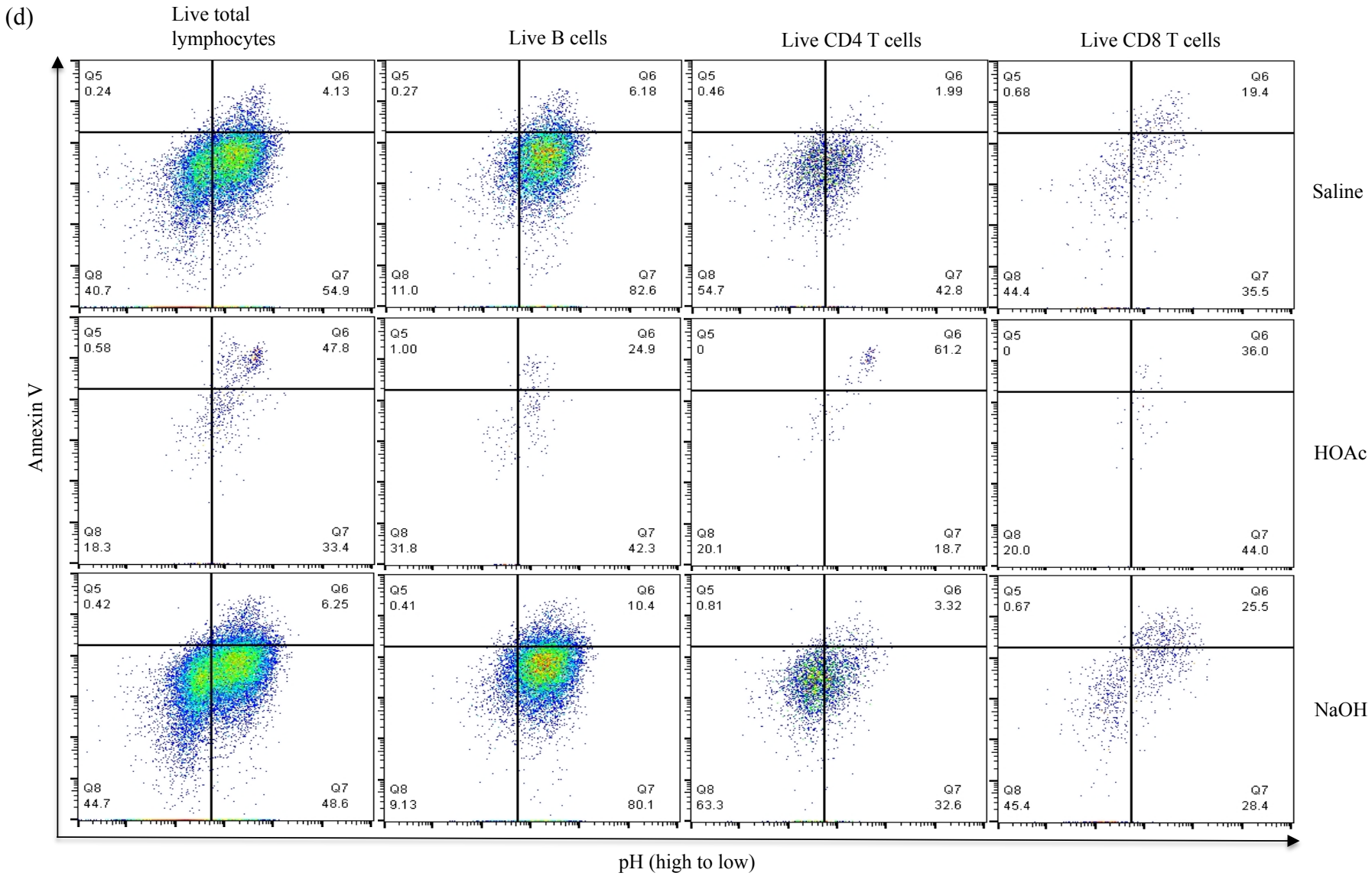
(d)
Live total lymphocytes
Live B cells
Live CD4 T cells
Live CD8 T cells
Saline
HOAc
NaOH
Annexin V
pH (high to low)
Q5 0.24
Q6 4.13
Q8 40.7
Q7 54.9
Q5 0.27
Q6 6.18
Q8 11.0
Q7 82.6
Q5 0.46
Q6 1.99
Q8 54.7
Q7 42.8
Q5 0.68
Q6 19.4
Q8 44.4
Q7 35.5
Q5 0.58
Q6 47.8
Q8 18.3
Q7 33.4
Q5 1.00
Q6 24.9
Q8 31.8
Q7 42.3
Q5 0
Q6 61.2
Q8 20.1
Q7 18.7
Q5 0
Q6 36.0
Q8 20.0
Q7 44.0
Q5 0.42
Q6 6.25
Q8 44.7
Q7 48.6
Q5 0.41
Q6 10.4
Q8 9.13
Q7 80.1
Q5 0.81
Q6 3.32
Q8 63.3
Q7 32.6
Q5 0.67
Q6 25.5
Q8 45.4
Q7 28.4

Figure 5d

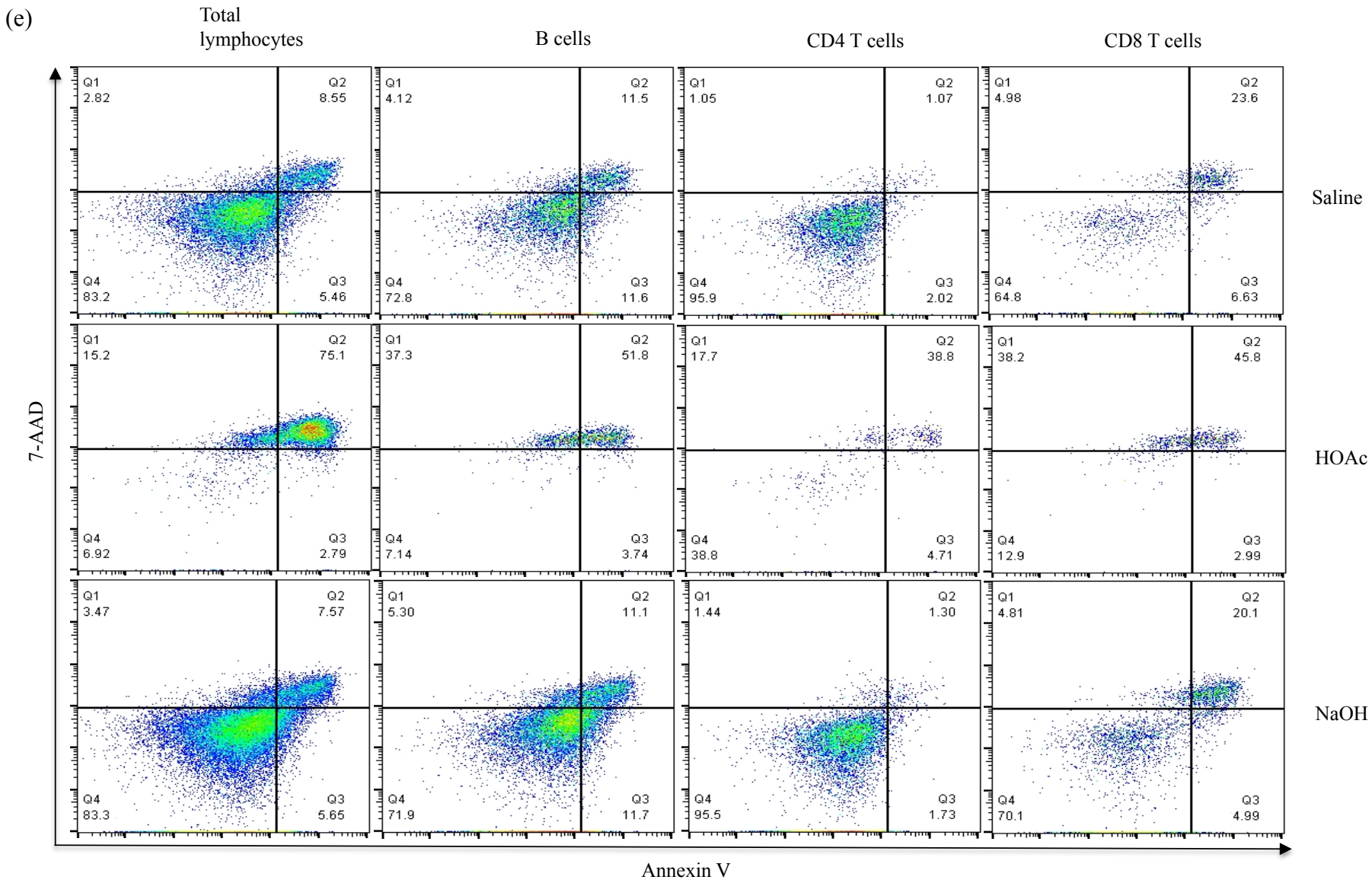
(e)
Total lymphocytes
B cells
CD4 T cells
CD8 T cells
Saline
HOAc
NaOH
7-AAD
Annexin V
Q1 2.82
Q2 8.55
Q4 83.2
Q3 5.46
Q1 4.12
Q2 11.5
Q4 72.8
Q3 11.6
Q1 1.05
Q2 1.07
Q4 95.9
Q3 2.02
Q1 4.98
Q2 23.6
Q4 64.8
Q3 6.63
Q1 15.2
Q2 75.1
Q4 6.92
Q3 2.79
Q1 37.3
Q2 51.8
Q4 7.14
Q3 3.74
Q1 17.7
Q2 38.8
Q4 38.8
Q3 4.71
Q1 38.2
Q2 45.8
Q4 12.9
Q3 2.99
Q1 3.47
Q2 7.57
Q4 83.3
Q3 5.65
Q1 5.30
Q2 11.1
Q4 71.9
Q3 11.7
Q1 1.44
Q2 1.30
Q4 95.5
Q3 1.73
Q1 4.81
Q2 20.1
Q4 70.1
Q3 4.99

Figure 5e

(f)

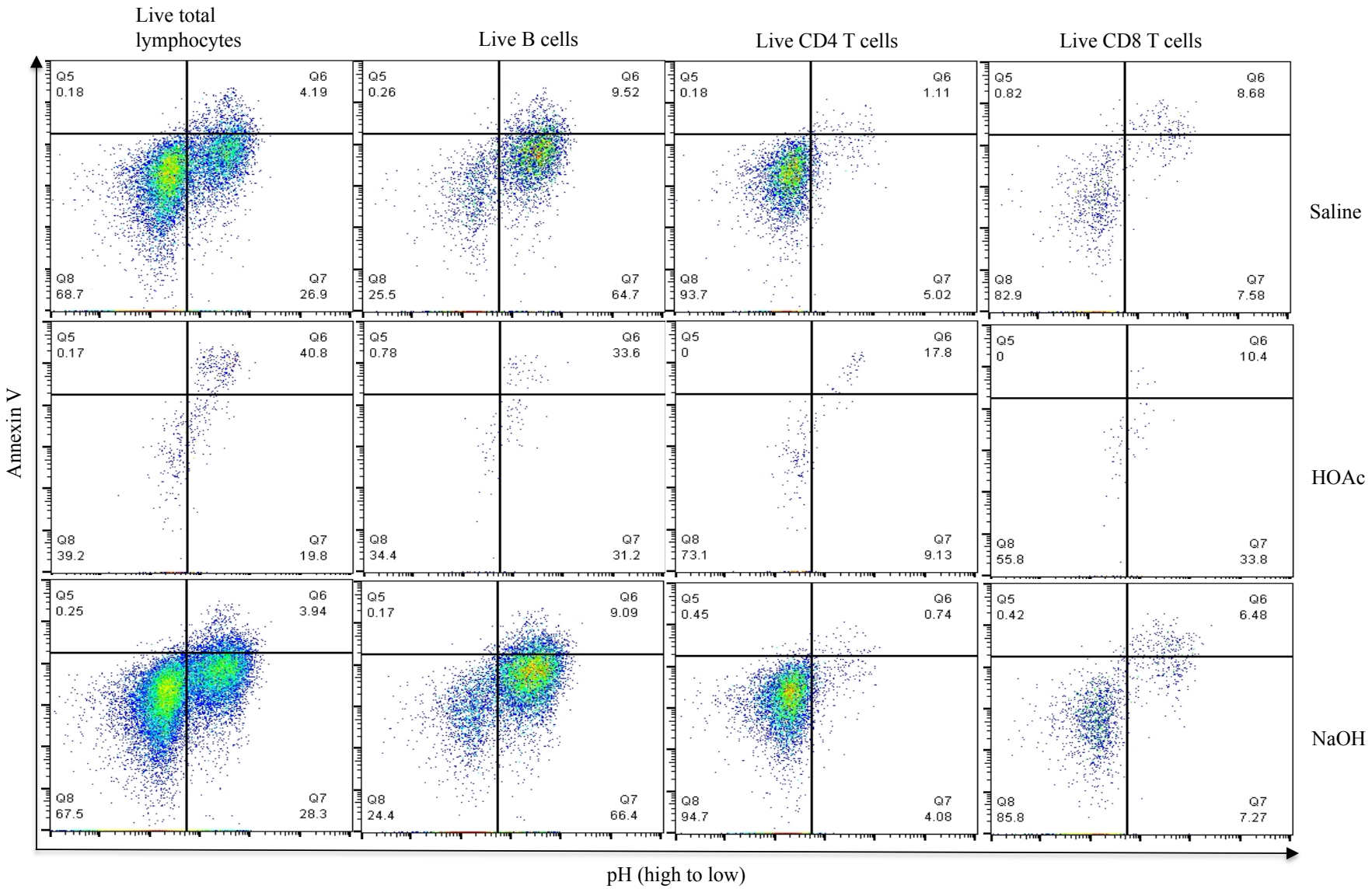
Live total lymphocytes
Live B cells
Live CD4 T cells
Live CD8 T cells
Saline
HOAc
NaOH
Annexin V
pH (high to low)
Q5 0.18
Q6 4.19
Q8 68.7
Q7 26.9
Q5 0.26
Q6 9.52
Q8 25.5
Q7 64.7
Q5 0.18
Q6 1.11
Q8 93.7
Q7 5.02
Q5 0.82
Q6 8.68
Q8 82.9
Q7 7.58
Q5 0.17
Q6 40.8
Q8 39.2
Q7 19.8
Q5 0.78
Q6 33.6
Q8 34.4
Q7 31.2
Q5 0
Q6 17.8
Q8 73.1
Q7 9.13
Q5 0
Q6 10.4
Q8 55.8
Q7 33.8
Q5 0.25
Q6 3.94
Q8 67.5
Q7 28.3
Q5 0.17
Q6 9.09
Q8 24.4
Q7 66.4
Q5 0.45
Q6 0.74
Q8 94.7
Q7 4.08
Q5 0.42
Q6 6.48
Q8 85.8
Q7 7.27

Figure 5f

(g)

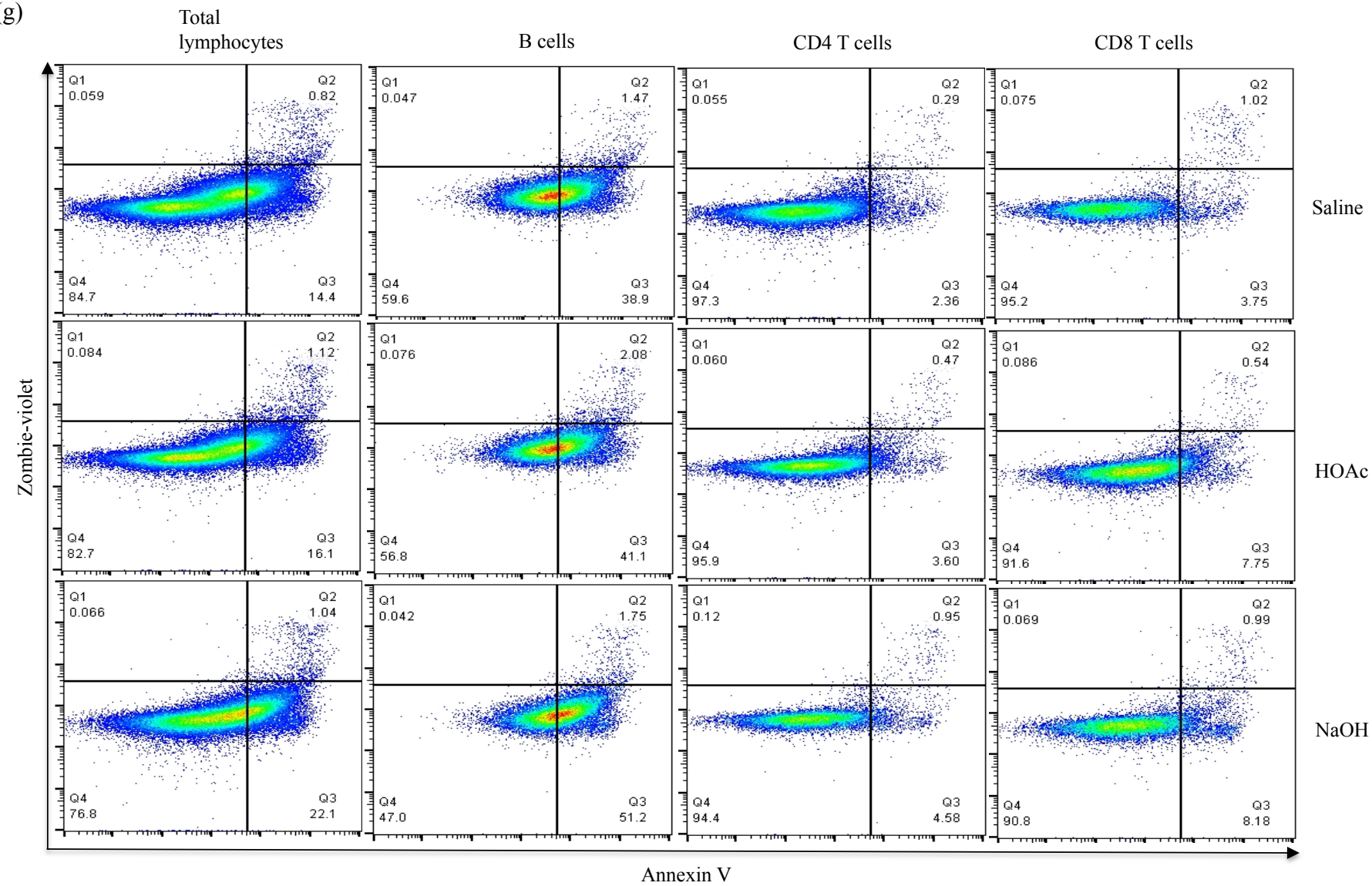
Total lymphocytes
B cells
CD4 T cells
CD8 T cells
Saline
HOAc
NaOH
Zombie-violet
Annexin V
Q1 0.059
Q2 0.82
Q4 84.7
Q3 14.4
Q1 0.047
Q2 1.47
Q4 59.6
Q3 38.9
Q1 0.055
Q2 0.29
Q4 97.3
Q3 2.36
Q1 0.075
Q2 1.02
Q4 95.2
Q3 3.75
Q1 0.084
Q2 1.12
Q4 82.7
Q3 16.1
Q1 0.076
Q2 2.08
Q4 56.8
Q3 41.1
Q1 0.060
Q2 0.47
Q4 95.9
Q3 3.60
Q1 0.086
Q2 0.54
Q4 91.6
Q3 7.75
Q1 0.066
Q2 1.04
Q4 76.8
Q3 22.1
Q1 0.042
Q2 1.75
Q4 47.0
Q3 51.2
Q1 0.12
Q2 0.95
Q4 94.4
Q3 4.58
Q1 0.069
Q2 0.99
Q4 90.8
Q3 8.18

Figure 5g

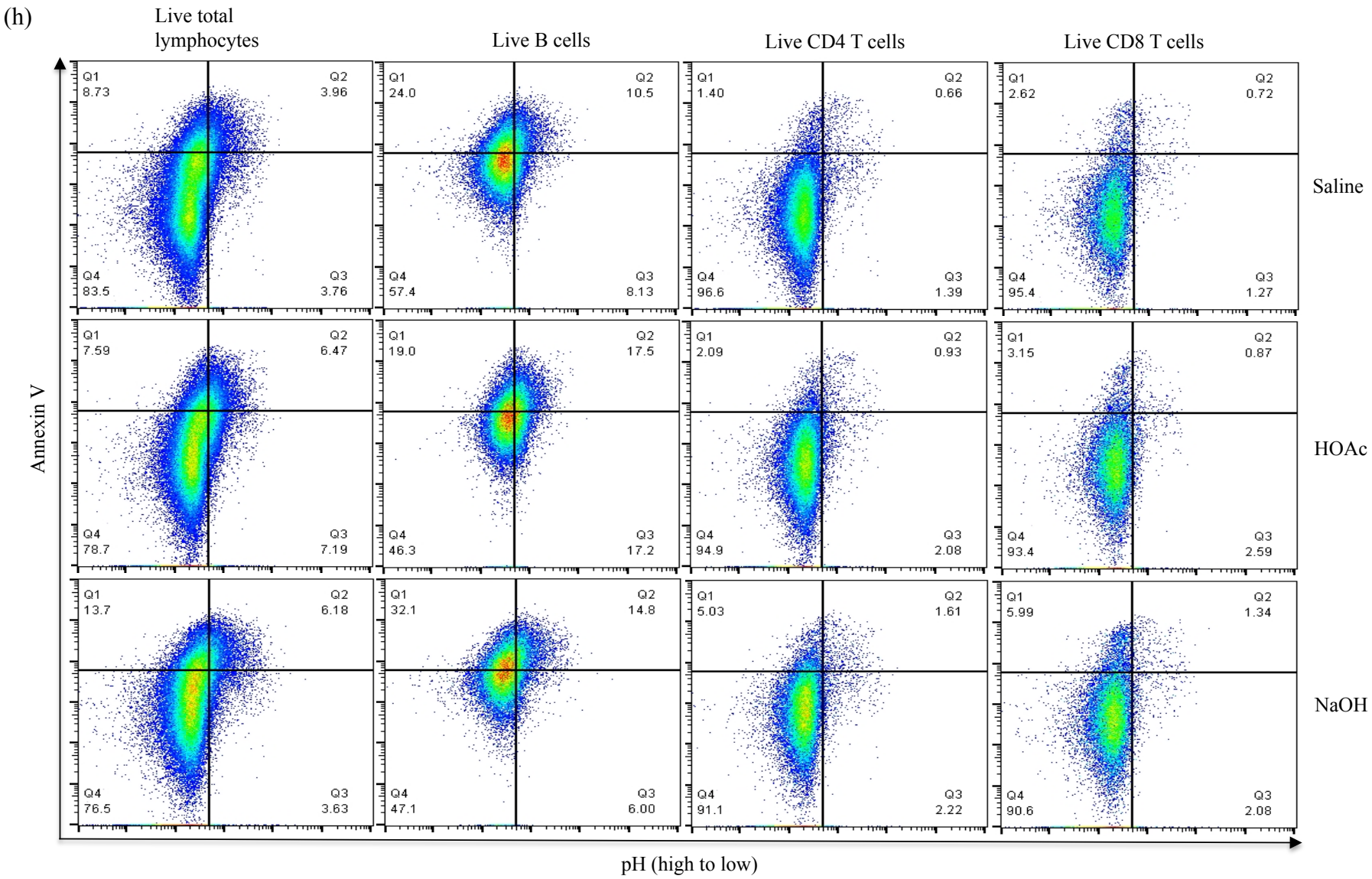
(h)
Live total lymphocytes
Live B cells
Live CD4 T cells
Live CD8 T cells
Saline
HOAc
NaOH
Annexin V
pH (high to low)
Q1 8.73
Q2 3.96
Q4 83.5
Q3 3.76
Q1 24.0
Q2 10.5
Q4 57.4
Q3 8.13
Q1 1.40
Q2 0.66
Q4 96.6
Q3 1.39
Q1 2.62
Q2 0.72
Q4 95.4
Q3 1.27
Q1 7.59
Q2 6.47
Q4 78.7
Q3 7.19
Q1 19.0
Q2 17.5
Q4 46.3
Q3 17.2
Q1 2.09
Q2 0.93
Q4 94.9
Q3 2.08
Q1 3.15
Q2 0.87
Q4 93.4
Q3 2.59
Q1 13.7
Q2 6.18
Q4 76.5
Q3 3.63
Q1 32.1
Q2 14.8
Q4 47.1
Q3 6.00
Q1 5.03
Q2 1.61
Q4 91.1
Q3 2.22
Q1 5.99
Q2 1.34
Q4 90.6
Q3 2.08

Figure 5h

(i)

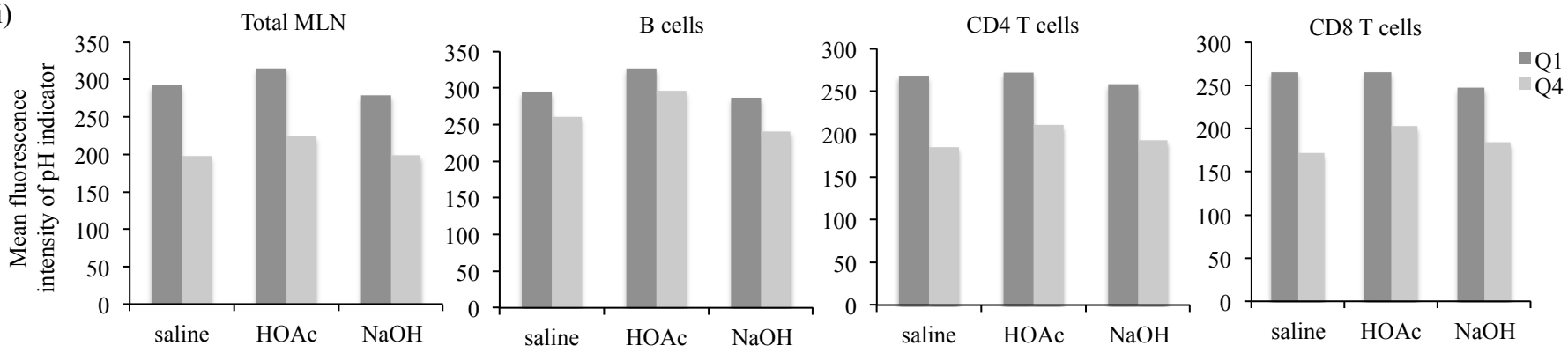
Total MLN
B cells
CD4 T cells
CD8 T cells
Mean fluorescence intensity of pH indicator
350
300
250
200
150
100
50
0
saline
HOAc
NaOH
Q1
Q4

Figure 5i

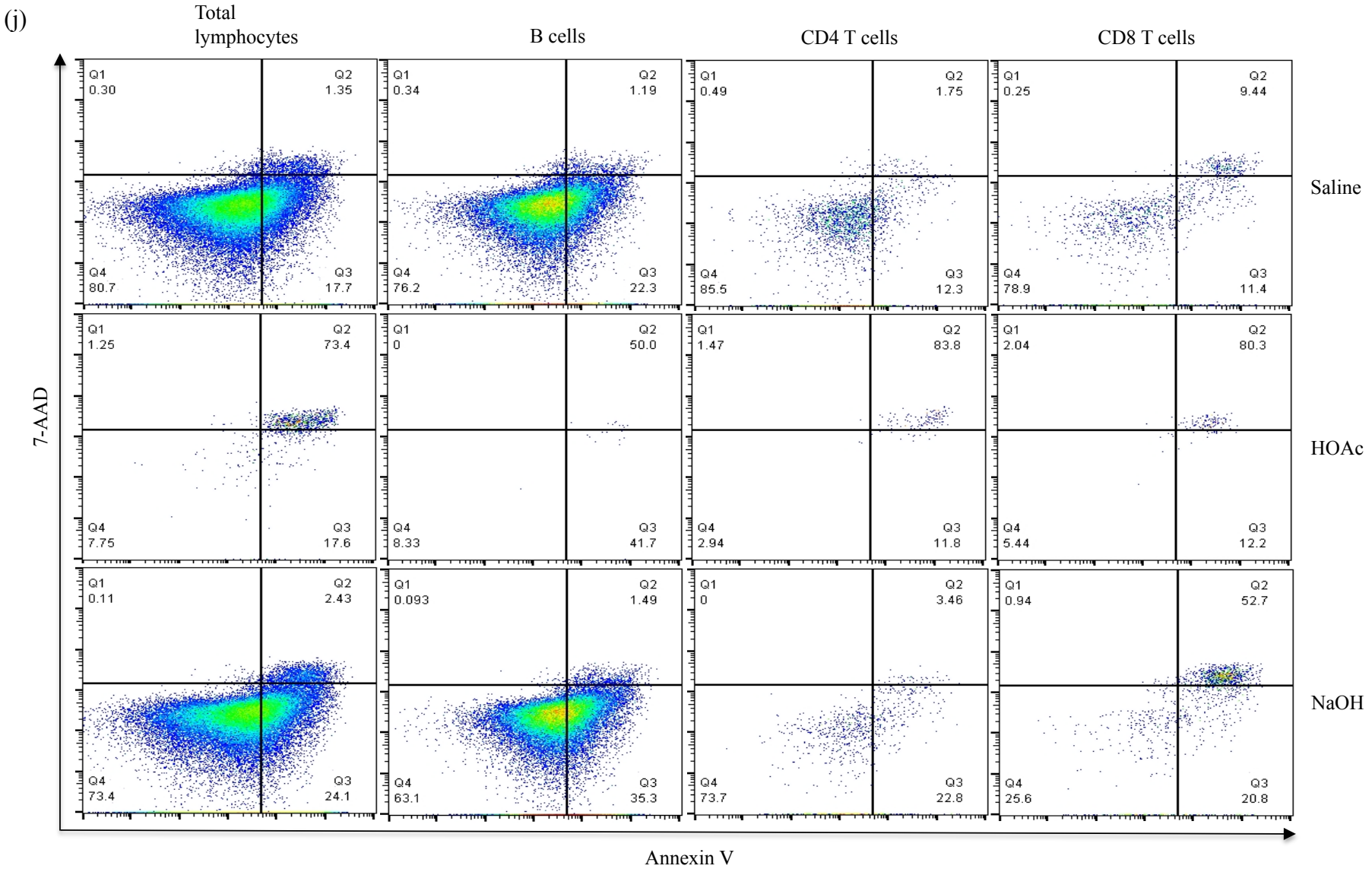
(j)
Total lymphocytes
B cells
CD4 T cells
CD8 T cells
Saline
HOAc
NaOH
7-AAD
Annexin V
Q1 0.30
Q2 1.35
Q4 80.7
Q3 17.7
Q1 0.34
Q2 1.19
Q4 76.2
Q3 22.3
Q1 0.49
Q2 1.75
Q4 85.5
Q3 12.3
Q1 0.25
Q2 9.44
Q4 78.9
Q3 11.4
Q1 1.25
Q2 73.4
Q4 7.75
Q3 17.6
Q1 0
Q2 50.0
Q4 8.33
Q3 41.7
Q1 1.47
Q2 83.8
Q4 2.94
Q3 11.8
Q1 2.04
Q2 80.3
Q4 5.44
Q3 12.2
Q1 0.11
Q2 2.43
Q4 73.4
Q3 24.1
Q1 0.093
Q2 1.49
Q4 63.1
Q3 35.3
Q1 0
Q2 3.46
Q4 73.7
Q3 22.8
Q1 0.94
Q2 52.7
Q4 25.6
Q3 20.8

Figure 5j

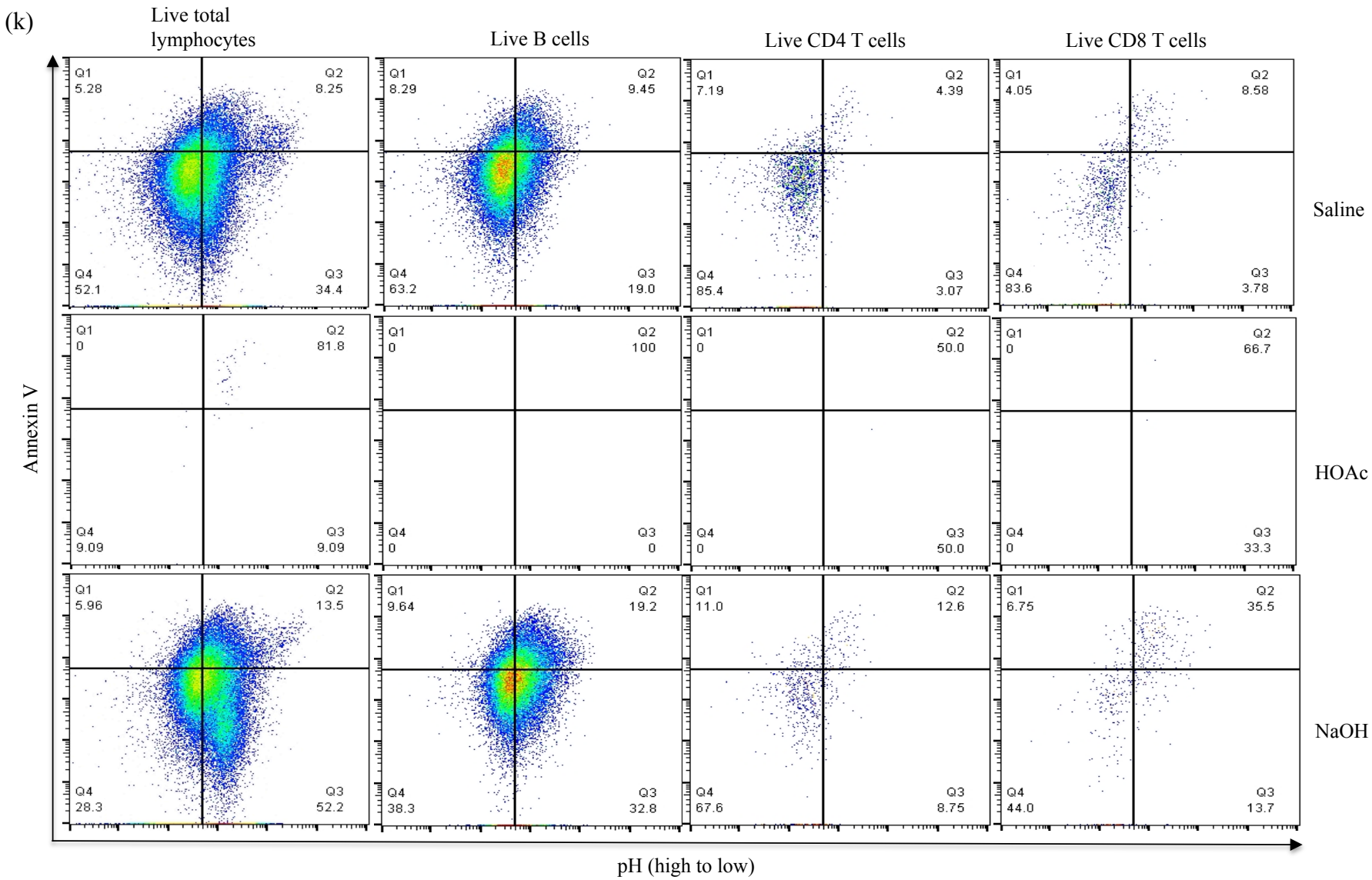
(k)
Live total lymphocytes
Live B cells
Live CD4 T cells
Live CD8 T cells
Saline
HOAc
NaOH
Annexin V
pH (high to low)
Q1 5.28
Q2 8.25
Q4 52.1
Q3 34.4
Q1 8.29
Q2 9.45
Q4 63.2
Q3 19.0
Q1 7.19
Q2 4.39
Q4 85.4
Q3 3.07
Q1 4.05
Q2 8.58
Q4 83.6
Q3 3.78
Q1 0
Q2 81.8
Q4 9.09
Q3 9.09
Q1 0
Q2 100
Q4 0
Q3 0
Q1 0
Q2 50.0
Q4 0
Q3 50.0
Q1 0
Q2 66.7
Q4 0
Q3 33.3
Q1 5.96
Q2 13.5
Q4 28.3
Q3 52.2
Q1 9.64
Q2 19.2
Q4 38.3
Q3 32.8
Q1 11.0
Q2 12.6
Q4 67.6
Q3 8.75
Q1 6.75
Q2 35.5
Q4 44.0
Q3 13.7

Figure 5k

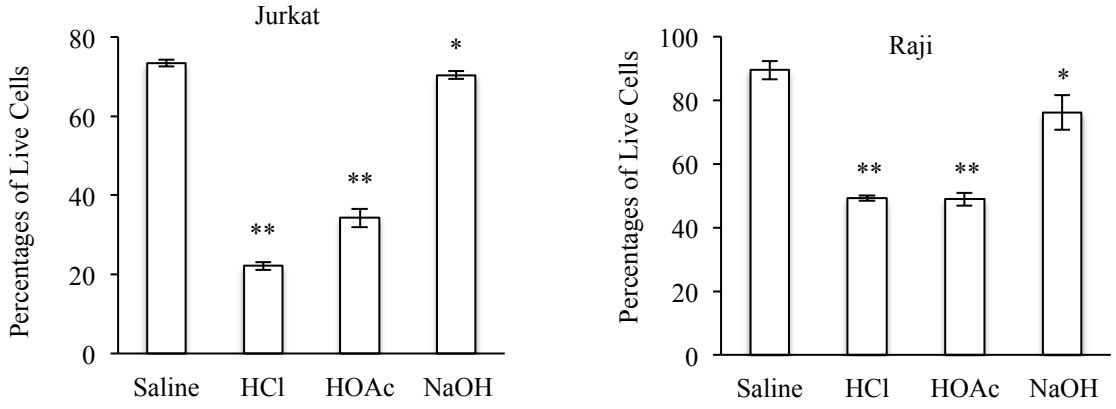
Jurkat
Percentages of Live Cells
80
60
40
20
0
**
**
*
Saline
HCl
HOAc
NaOH
Raji
Percentages of Live Cells
100
80
60
40
20
0
**
**
*
Saline
HCl
HOAc
NaOH

Figure 6a

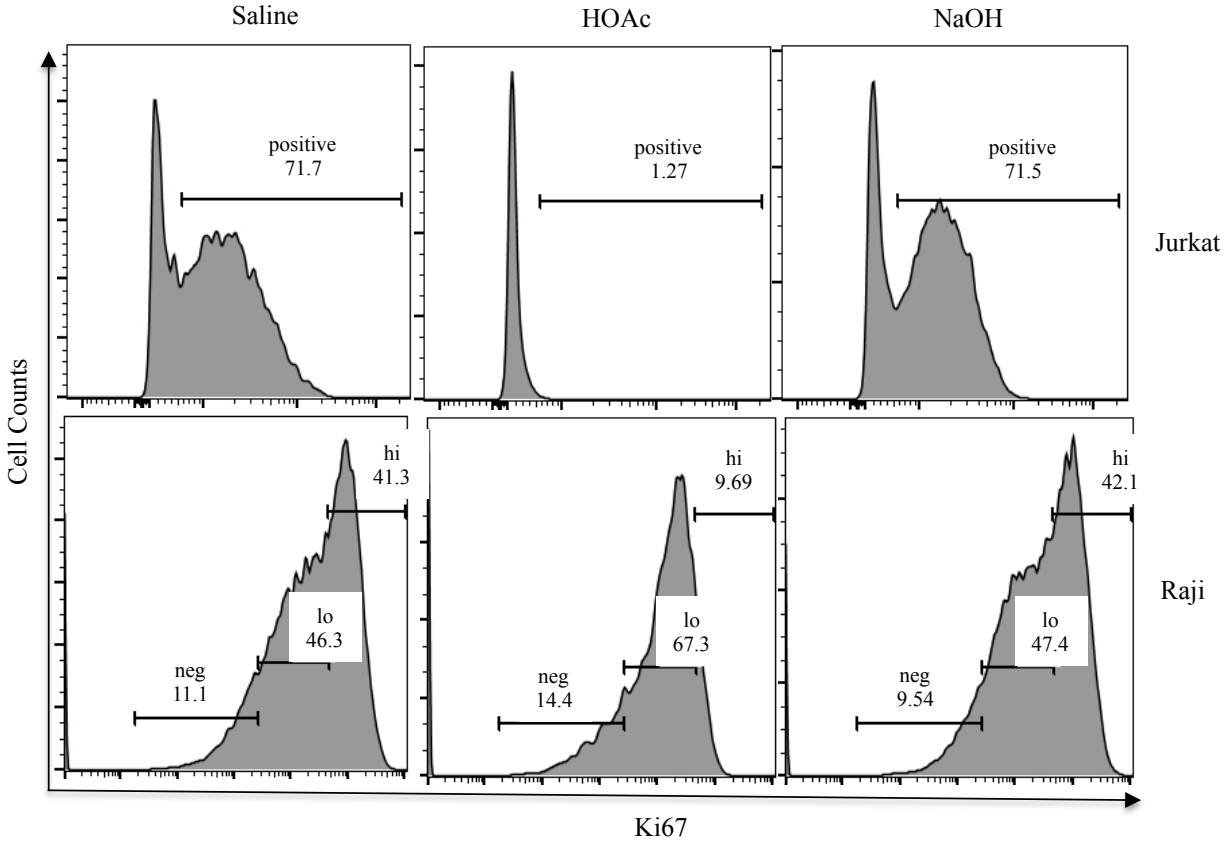
Saline
HOAc
NaOH
positive
71.7
positive
1.27
positive
71.5
Jurkat
Cell Counts
hi
41.3
lo
46.3
neg
11.1
hi
9.69
lo
67.3
neg
14.4
hi
42.1
lo
47.4
neg
9.54
Raji
Ki67

Figure 6b

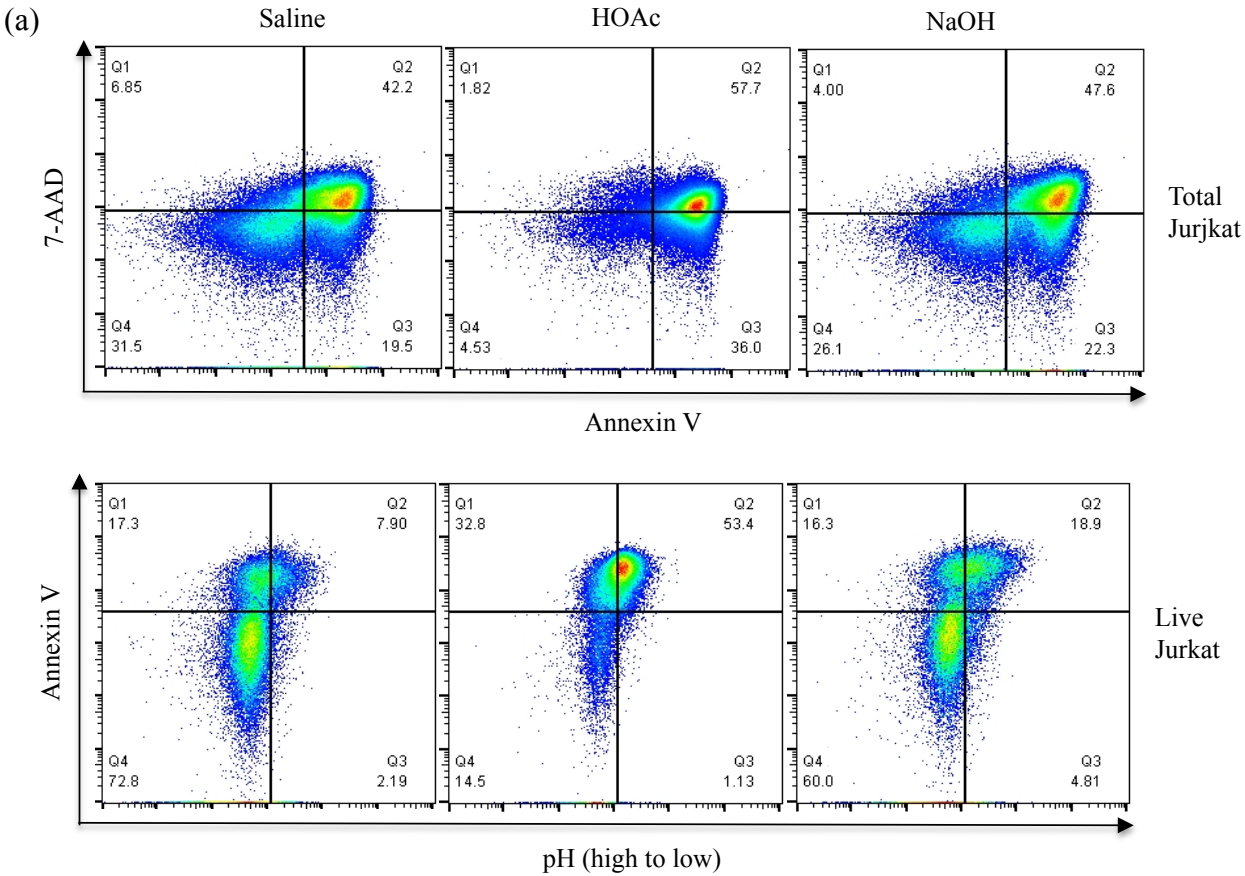
(a)
Saline
HOAc
NaOH
7-AAD
Q1
6.85
Q2
42.2
Q4
31.5
Q3
19.5
Q1
1.82
Q2
57.7
Q4
4.53
Q3
36.0
Q1
4.00
Q2
47.6
Q4
26.1
Q3
22.3
Total
Jurjkat
Annexin V
Annexin V
Q1
17.3
Q2
7.90
Q4
72.8
Q3
2.19
Q1
32.8
Q2
53.4
Q4
14.5
Q3
1.13
Q1
16.3
Q2
18.9
Q4
60.0
Q3
4.81
Live
Jurkat
pH (high to low)

Figure 7a

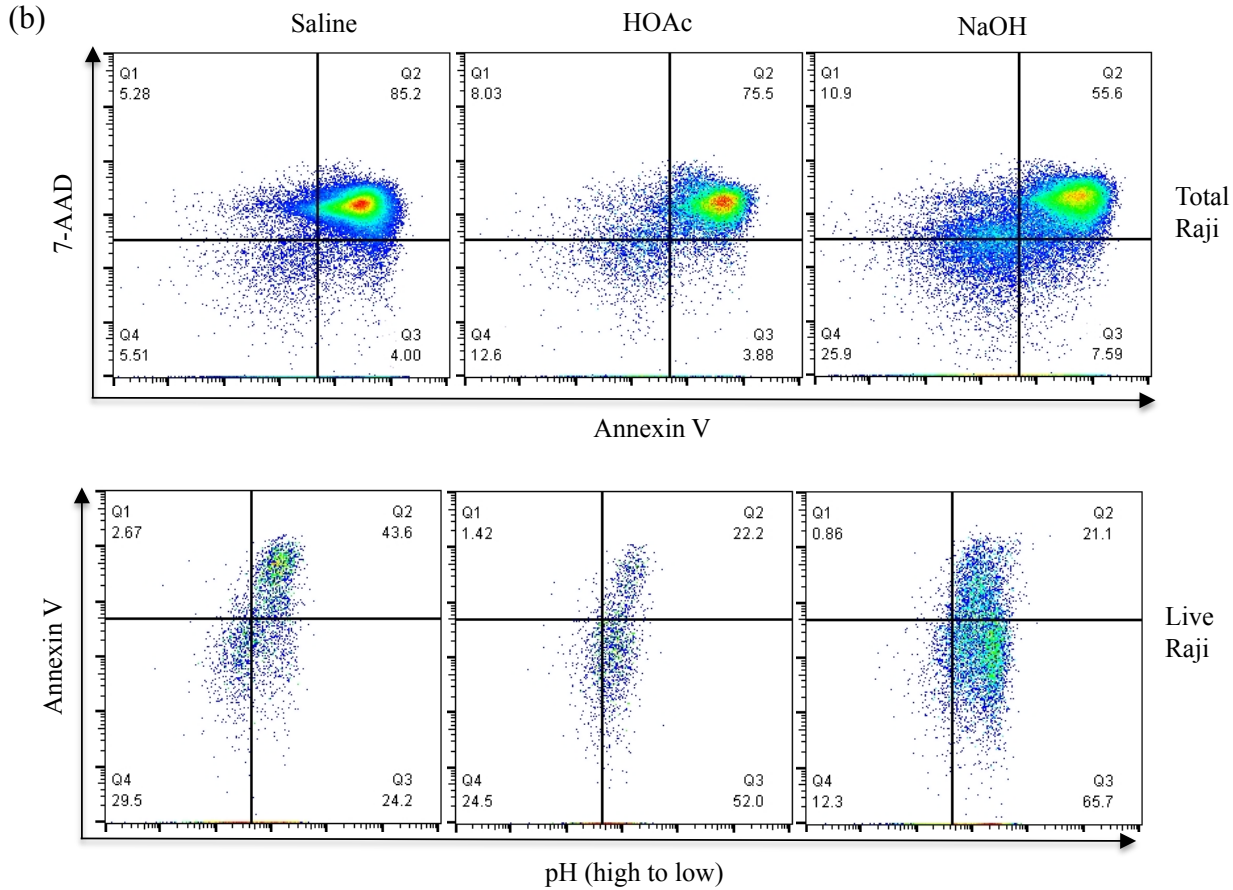
(b)
Saline
HOAc
NaOH
7-AAD
Q1
5.28
Q2
85.2
Q4
5.51
Q3
4.00
Q1
8.03
Q2
75.5
Q4
12.6
Q3
3.88
Q1
10.9
Q2
55.6
Q4
25.9
Q3
7.59
Total
Raji
Annexin V
Annexin V
Q1
2.67
Q2
43.6
Q4
29.5
Q3
24.2
Q1
1.42
Q2
22.2
Q4
24.5
Q3
52.0
Q1
0.86
Q2
21.1
Q4
12.3
Q3
65.7
Live
Raji
pH (high to low)

Figure 7b